1953

The niobium-thorium and the niobium-vanadium alloy systems

James M. Dickinson
Iowa State College

NOTE TO USERS

Title: The Niobium-Therium and the Niobium-Vanadium Alloy System

Author: James M. Dickinson

(Official certification of the classification shown is filed in the Ames Laboratory Document Library)

Signature was redacted for privacy.

Secretary to Declassification Committee

THE NIOBIUM-THORIUM AND THE NIOBIUM-VANADIUM ALLOY SYSTEMS

by

James M. Dickinson

A Dissertation Submitted to the
Graduate Faculty in Partial Fulfillment of
The Requirements for the Degree of
DOCTOR OF PHILOSOPHY

Major Subject: Physical Chemistry

Approved:

Signature was redacted for privacy.

In Charge of Major Work

Signature was redacted for privacy.

Head of Major Department

Signature was redacted for privacy.

Dean of Graduate College

Iowa State College
1953

TABLE OF CONTENTS

I. INTRODUCTION

The investigations of the niobium-thorium and the niobium-vanadium binary alloy systems were undertaken primarily to establish their phase diagrams.

Since both alloy systems contain refractory metals, the determination of the phase diagrams was expected to present considerable experimental difficulties. To suggest an approach for the experimental determination of the phase diagrams and to later allow a comparison of the predicted and the experimentally determined phase diagrams, a survey of the factors involved in alloying was undertaken.

The parameters usually employed in such preliminary surveys are the atomic radius, the electronegativity of the metal, and the solubility parameter. The values of these parameters for the elements involved are listed in Table 1. Two sets of values are listed for both the electronegativity and the atomic radius. Pauling's (1) values of the metallic radii are based upon the coordination number of twelve since most metals have closest packed structures. The values tabulated as atomic radii are one-half the distance of closest

approach of the atoms and were calculated from the dimensions of the particular unit cell involved. One set of values of the electronegativities was calculated using Pauling's (2) electronegativity equation

$$Q = (23.06)\ (x_a - x_o)^2 \qquad (1)$$

where Q is the heat of formation for the reaction and x represents the electronegativity of the species involved. The other set of values was taken from a tabulation made by Oraini (3) using Gordy's (4) equation

$$X = \frac{0.31(n-1)}{r_c} \quad 0.50 \qquad (2)$$

where n is the valence, r_c the single bond covalent radius or, if this is not available, the metallic radius, and X is the electronegativity of the metal.

Table 1. Parameters Useful for the Prediction of Alloy Systems

Element	Radius		Electronegativity		Hildebrand's solubility parameter
	Metallic	Atomic	Pauling's	Gordy's	
V	1.338	1.32	1.8	1.891	119
Nb	1.456	1.43	1.9	1.779	127
Th	1.795	1.82	1.3	1.364	125

The percentile difference between the electronegativities of two elements is given by the equation

$$X = \frac{100(x_1 - x_2)}{x_{avg.}} \qquad (3)$$

where X is the percentile difference of electronegativities, x_1 and x_2 are the electronegativities of the elements, and $x_{avg.}$ is the arithmetic mean of x_1 and x_2. The percentile difference between the atomic radii of two elements is given by the equation

$$R = \frac{100(r_1 - r_2)}{r_{avg.}} \qquad (4)$$

where r_1 and r_2 are the radii of the elements and R is the percentile difference of the atomic radii. The values of R and X for the niobium-thorium and the niobium-vanadium alloy systems are listed in Table 2.

Table 2. Difference of Atomic Radii and Electronegativities

Alloy System	R		X	
	Metallic	Atomic	Pauling's	Gordy's
Nb-Th	20.85	24	37.5	26.4
Nb-V	8.4	8	5.4	6.1

It has been shown by Hume-Rothery (5) that if the difference in atomic radii of two metals is less than 15 per cent and if the electronegativities are similar i.e., the percentile difference is small, that complete solid solution may occur. Also, it has been shown (6) that if a complete solid solution is formed and the difference in atomic radii is more than 8 per cent it is probable that a minimum is formed in the solidus curve.

It is apparent, on the basis of the data tabulated in Table 2,

that complete solid solution may occur in the niobium-vanadium alloy system, and it is just as apparent that complete solid solution should not occur in the niobium-thorium alloy system. Since the difference in electronegativities between niobium and thorium is quite large, the formation of intermediate phases might be expected. However, the examination of a large number of alloy systems tabulated by Oraini (3) indicates that this system is a borderline case as far as the formation of intermediate phases is concerned. There remains then the possibility that the niobium-thorium alloy system might show liquid immiscibility. Hildebrand (7) has developed a method of relating properties of metals and liquid immiscibility. For liquid immiscibility to occur the following equation should hold:

$$\frac{(V_1 + V_2)}{2}(\delta_1 - \delta_2)^2 > 2RT. \qquad (5)$$

V is the atomic volume i.e., the atomic weight divided by the density, T is the absolute temperature, and R is the gas constant expressed in calories per mole degree. δ has been defined by Hildebrand as

$$\delta = \left(\frac{\Delta E^V}{V_\ell}\right)^{\frac{1}{2}} \qquad (6)$$

where ΔE^V is the energy of vaporization and V_ℓ is the molar volume of the liquid. If the vapor is assumed to act as a perfect gas, equation (6) may be written

$$\delta = \left(\frac{\Delta H^V - RT}{V_\ell}\right)^{\frac{1}{2}} \qquad (7)$$

where ΔH^V is the heat of vaporization of the liquid. If the value of

ΔH^V is not readily available it may be approximated using the relationship developed by Scott (8)

$$\Delta H^V = 17T_b + 0.009T_b \ldots\ldots \quad (8)$$

Hildebrand (7) has shown both theoretically and experimentally that for metals δ does not vary appreciably with temperature so that it is a good approximation to use the value of δ calculated at the boiling point at any temperature. Since neither the boiling point nor the heat of vaporization is accurately known for thorium, the value of δ for thorium that had been estimated by Carlson (9) was used. This value was estimated by a comparison of the melting points of metals and their δ values, and in at least one case, the thorium-uranium system, a calculation based on the estimated δ value for thorium correctly predicted liquid immiscibility.

Using the δ values listed in Table 1, a calculation of the possibility of the occurrence of liquid immiscibility in the niobium-thorium system at 1000°K. was made. For liquid immiscibility to occur the following equation should hold:

$$\left(\frac{V_{Nb} + V_{Th}}{2}\right)\left(\delta_{Nb} - \delta_{Th}\right)^2 > 2RT. \quad (9)$$

Upon substituting numerical values we find

$$\left(\frac{10.95 + 19.83}{2}\right)(127 - 125)^2 < (2)(2)(1000) \quad (10)$$

$$61.6 < 4000. \quad (11)$$

Since the value of the right hand side of equation (11) is much larger than the left hand side of the equation, liquid immiscibility should

not occur.

The following predictions can now be made for the two alloy systems of interest:

1. The niobium-thorium alloy system should be a eutectic type system with little or no terminal solid solubility and there is a possibility that intermediate phases may be formed.

2. The niobium-vanadium alloy system should form a complete series of solid solutions and the solidus curve of this system may pass through a minimum.

II. THE NIOBIUM-THORIUM ALLOY SYSTEM

A. Historical

The element niobium, formerly called columbium, was discovered in 1801 by Hatchett (10). Niobium metal was first prepared in 1864 by Blomstrand (11) who reduced the chloride with hydrogen. The principal mineral (12) of niobium is tantalite which is an impure solid solution of tantalum and niobium pentoxides. The separation of niobium and tantalum is a difficult and expensive operation due to their similar chemical properties. This, in conjunction with the scarcity of tantalite, accounts for the present high price, 85 to 150 dollars per pound, of niobium.

Niobium is a bright shiny metal that is very malleable and ductile. Niobium has an atomic weight of 92.12, an atomic number of 41, and a density of 8.57 grams per cubic centimeter (13). It is a body-centered cubic metal and has a lattice constant of 3.308 Angstroms (14). Melting points ranging from 1950 (15) to 2500°C. (16) have been reported. The best value of the melting point is probably 2415°C. (14).

The element thorium was discovered by Berzelius (17) in 1828. The principal mineral of thorium is monazite (18). Thorium is a soft silver-white metal that tarnishes slowly upon exposure to air. It has an atomic weight of 232.12, an atomic number of 90, and a density of about 11.7 grams per cubic centimeter varying slightly depending upon the method of preparation and fabrication (19). Melting points ranging from 1450 to 1842°C. have been reported for thorium. The

best value of the melting point is probably about 1695°C. (20). At room temperature the stable form of thorium is face-centered cubic with a lattice constant of 5.087 Angstroms (19). Small additions of carbon have been shown to raise the lattice constant of thorium sharply (21). An allotropic form of thorium has recently been identified by Chiotti (22) using a high temperature X-ray diffraction method. The high temperature form exists above 1400°C. and is body-centered cubic having a lattice constant of 4.11 Angstroms.

A thorough search of both classified and unclassified literature failed to reveal that any systematic study of the niobium-thorium alloy system had been made. Several investigators have studied the fabrication and mechanical properties of niobium-thorium alloys containing less than 2 per cent niobium. Goldhoff (23) reported that these alloys could be forged or rolled at 700°C. and that they could be cold rolled. He also found that the addition of 0.4 per cent niobium to thorium increased the tensile strength of thorium slightly. Frye (24) reported that the addition of less than 4 per cent niobium to thorium decreased the hardness of the alloy. Rogers (25) reported that the ultimate tensile strength of a 2 per cent niobium alloy was 55,000 psi. and that the same alloy had a Brinell hardness number of 95. Foote (26) reported a eutectic at 1315°C. in the thorium rich region of the alloy system.

B. Apparatus and Experimental Methods

1. Preparation of alloys

Most of the alloys studied during the course of this investigation were prepared from niobium powder obtained from the Fansteel Metallurgical Corporation and from thorium sponge prepared for experimental purposes at this laboratory. A few alloys were made using trimmings from niobium sheet that was also obtained from Fansteel. The major impurity in both thorium and niobium was carbon. Powdered niobium contained about 1760 ppm. carbon, sheet niobium contained less than 500 ppm. carbon, and the thorium contained less than 460 ppm. carbon. Minor amounts of calcium, chromium, iron, magnesium, silicon, titanium, vanadium, and zirconium were detected in the niobium by spectrographic analysis. The thorium contained less than 100 ppm. of iron, calcium, zinc, or aluminum. No oxygen analyses were obtained on either metal.

Thorium sponge was prepared for melting by breaking it into small lumps approximately one-half inch in diameter. The niobium powder was pressed into flat disks weighing one to ten grams. Enough metal was prepared in this manner to make all the alloys needed for this investigation. By randomly selecting the metals needed for alloy preparation from these small pieces, the variation of impurity content between samples was minimized.

The alloys were prepared by melting the required amounts of niobium and thorium together in an arc melting furnace designed for

small scale experimental melting. The arc melter was conventional in design having a removable copper melting crucible that served as the positive electrode and a water cooled tungsten rod for the negative electrode. The arc melting chamber was evacuated to a pressure of less than 5×10^{-5} millimeters of mercury and filled with highly purified helium. This process was repeated three times. A piece of zirconium, perhaps 20 or 30 grams, was then melted in the gas filled chamber to remove any remaining impurities in the helium. Each alloy was melted four times before removing it from the arc melting chamber. Between each melting the alloy was turned over with the tungsten electrode to insure good mixing. Alloys prepared from niobium sheet were melted in the same manner.

Several of the alloys were reduced 50 to 75 per cent by cold rolling and then annealed in vacuo at 1000°C. for 48 hours. No change in the microstructure of these alloys was observed, so that normally only non-homogeneous appearing alloys were given this homogenization treatment.

2. Metallographic procedure

Alloys containing less than 90 per cent niobium were prepared for microscopic examination by rough grinding a flat surface on the sample followed by grinding on silicon carbide grinding papers of successively decreasing grit sizes. The final grinding operation was carried out on Tri-M-ite 600 A grinding paper. Since the surface of the specimen smeared badly during the grinding operations it was often helpful

to electrolytically polish the specimen between grinding operations to remove the worked metal.

The polishing operation that gave the best results was a combination of mechanical and electrolytic polishing. Alloys were alternately polished on a microcloth covered wheel using a soap suspension of 600 grit silicon carbide powder as an abrasive and electrolytically polished in a 3 N nitric acid bath containing 1 per cent potassium fluoride. The current density was varied between one and four amperes per square centimeter, and the polishing time was varied between fifteen and sixty second depending upon the reactivity of the samples. Samples containing 5 to 9 per cent niobium were the most reactive and required lower current densities and shorter polishing times. Alloy surfaces prepared in this manner were free of scratches and worked metal.

The polished specimens were electrolytically etched in the electrolyte used for polishing. The current density was varied between 20 and 300 milliamperes per square centimeter, and the etching time was varied between five and sixty seconds depending upon the reactivity of the specimen in the same manner as in the polishing operation. Often a thin film was formed on the sample during the etching process. If continued etching failed to remove the film, it often could be removed by gently rubbing the surface of the specimen with Kleenex saturated with alcohol.

Alloys containing over 95 per cent niobium generally needed no mechanical or electrolytic polishing. After grinding through Tri-M-ite 600 A grit paper they were chemically polished and etched in one

operation by immersing the specimen in aqua regia containing 5 per cent hydrofluoric acid for a few seconds. It was noticed that alloys made from the sheet niobium, which had a low carbon content, were very difficult to chemically polish. Normally some mechanical polishing was necessary to prepare scratch free surfaces on these alloys.

3. X-ray apparatus and methods

All of the X-ray diffraction patterns obtained during the course of this investigation were taken on a North American Philips water-cooled X-ray diffraction unit using copper K alpha radiation. A 114.7 millimeter diameter Debye-Scherrer type powder camera, a 120 millimeter self-focusing back-reflection camera, and a high temperature attachment mounted on a Norelco diffractometer were used to obtain the data reported in this paper.

Powdered specimens for use in the Debye-Scherrer and back-reflection cameras were prepared by filing the appropriate alloys. After screening the finely divided sample on a 150 mesh screen any iron contamination introduced during the filing operation was removed by passing a strong permanent magnet over the sample. A zirconium strip and the filings were placed in opposite ends of a 3 millimeter diameter quartz tube and the tube was sealed. By heating the end of the tube containing the zirconium strip at approximately 1000°C. for 15 minutes while cooling the end of the tube containing the filings in a beaker of cold water, a good vacuum was produced in the tube due to the "getter" action of the zirconium. The tube containing the X-ray

specimen was then annealed at 600 to 650°C. for 113 hours to remove residual stresses in the specimen.

A major source of error in cameras employing film has been shown to be film shrinkage (27). Since film does not always shrink uniformly, a correction should be made for both linear and nonlinear film

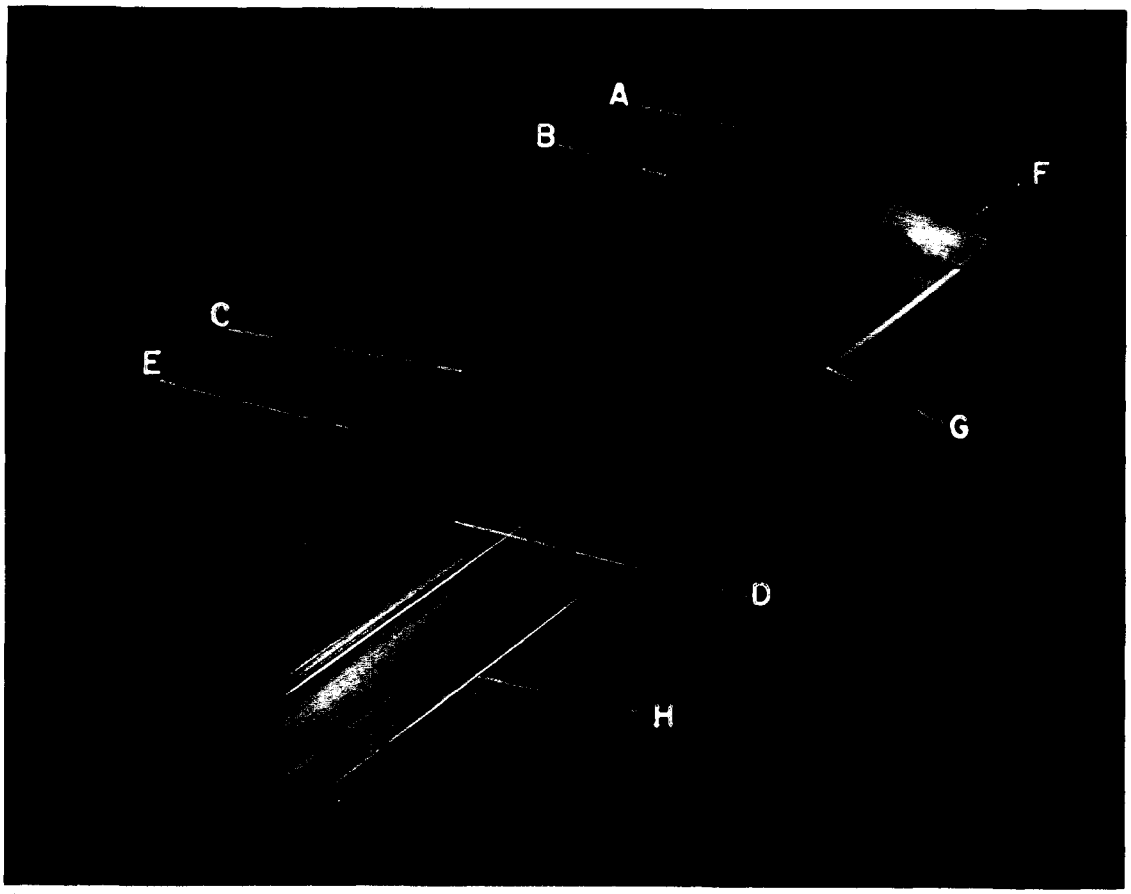

Fig. 1 Punch for Calibrating X-ray Film

shrinkage. A device to punch fiducial marks on the X-ray film was constructed to allow a correction to be made for nonlinear as well as linear film shrinkage. This punch, illustrated in Figure 1, punched small holes in the film at 2 ± 0.003 centimeter intervals. By

measuring the position of the holes after the film had been processed it was possible to correct accurately for film shrinkage. The punch was calibrated at regular intervals by measuring the position of the holes punched in an unprocessed film. The punch was constructed entirely of stainless steel, polished to a mirror finish, except for the strip of teflon (G) in the base (H) to protect the needle points. The plate (E), which has a row of small holes (C) drilled in it so that the needles may pass through the plate, has two purposes. It is held away from the top (A) by springs so that the phonograph needles used to make the holes are not protruding except when actually punching the holes. It also serves to push the film off the needles after the holes have been punched. Small set screws, which can be adjusted from the holes (B), hold the needles in place, and also provide an easy way to change needles if necessary. The film was pushed firmly against the shoulder (D) of the base and the end plate (F). The top of the punch was lowered until it made contact with the film, and then the top was given a hard push downward to punch the holes.

Three curves have been plotted in Figure 2 illustrating the types of film shrinkage that were experimentally observed. Curve (a) is essentially a straight line and indicates that the shrinkage was nearly linear. This particular film shrank over 0.3 centimeter during processing. Shrinkage of the films was recorded all the way from 0.025 to 0.5 centimeters. Curve (b) illustrates a rather unusual case in that most of the shrinkage occurred in one-half of the film. The curve (c) illustrates a case of rather pronounced nonlinear film

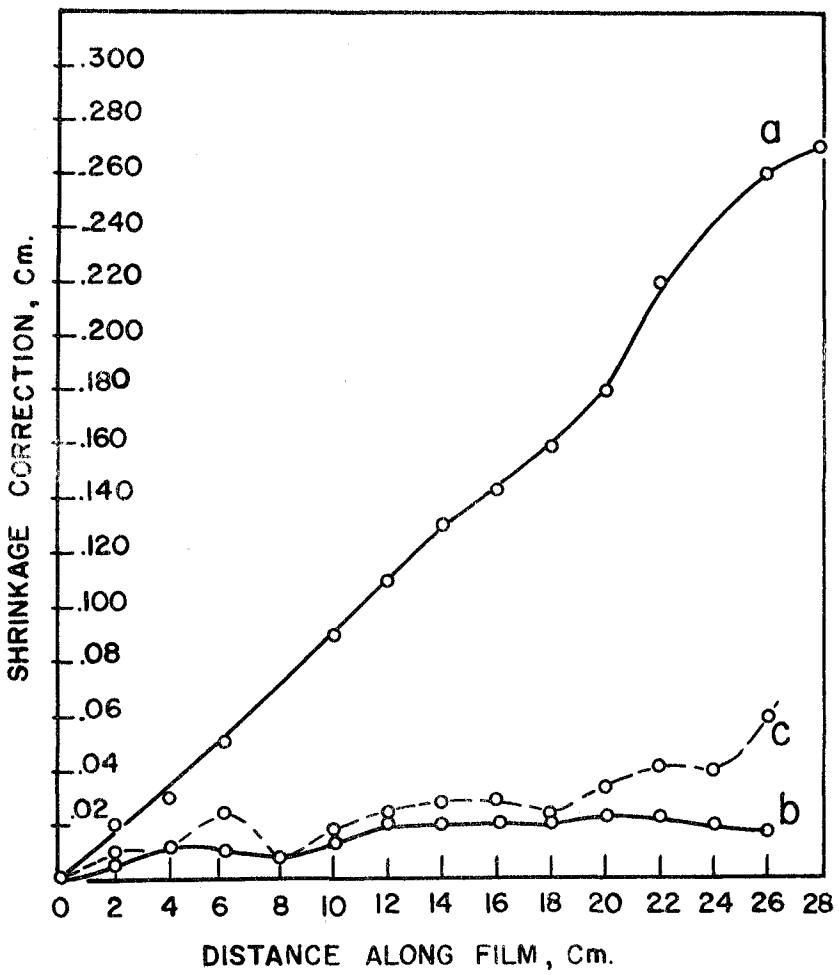

Fig. 2 Film Shrinkage Correction Curves.

shrinkage. The factors influencing film shrinkage are not too well understood but several conclusions can be reached. The films that underwent very little film shrinkage were measured the same day that they were developed, while most of those that shrank a great deal were stored for several days before being measured; so that, it appears that drying time plays an important part in determining the extent of film shrinkage. It was also noticed in several, but not all cases, that nonlinear shrinkage occurred near the large holes in the X-ray film.

High temperature X-ray studies were carried out using a special attachment designed by Chiotti (22) of this laboratory on a Norelco diffractometer. Briefly, the attachment consisted of a vacuum chamber containing a tantalum sheet resistance furnace and a thorium or carbon specimen holder. The vacuum chamber was provided with an aluminum foil window to allow passage of the X-ray beam. X-ray patterns could be obtained at temperatures as high as 1600°C. and at pressures from 2×10^{-6} to 5×10^{-5} millimeters of mercury using this equipment.

Specimens to be used for high temperature X-ray studies were prepared by milling slabs measuring 1/4 X 1/16 X 3/4 inches from arc melted alloys and polishing the samples in accordance with standard metallographic procedures. The polished specimen was mounted in the furnace and heated to a specific temperature where a portion of the front reflection region was scanned. The temperature was then raised 25 to 50°C. and the same portion of the front reflection region rescanned. This process was repeated until the temperature of the transformation was located. After the transformation temperature had

been determined, the front and back-reflection regions were normally scanned at a temperature just above and at a temperature just below the transformation temperature. Unfortunately, very few peaks were strong enough to be measured in the back-reflection region.

4. Methods of solidus determination

Three independent methods were used to determine the shape of the solidus curve. These methods involved cooling curves, melting-bar techniques and high temperature resistance measurements.

(a) Cooling curves. Under favorable conditions cooling curves have been one of the most useful tools employed by metallurgists for the study of phase diagrams. Although the study reported in this investigation was an extremely unfavorable case, an attempt was made to obtain as much thermal data as was practical. Since thorium, due to its low heat of fusion, does not exhibit a measurable thermal arrest at its melting point, a very sensitive method of thermal analysis was necessary. Another complicating factor was the lack of a reliable thermocouple that would withstand temperatures above 1400°C. Platinum-platinum-13 per cent rhodium thermocouples became brittle when heated in a vacuum in the presence of carbon, so niobium-tungsten thermocouples were used. Niobium-tungsten thermocouples have several disadvantages but have the advantage of a very high temperature range. Tungsten wire becomes brittle upon heating and cannot be handled; consequently, a new thermocouple must be made each time the specimen is

changed. Moreover, the calibration of the thermocouple varies making it necessary to calibrate the thermocouple during each run. This was done by checking the temperature at regular intervals with a calibrated optical pyrometer while the cooling curve was being recorded.

Differential cooling curves employing a neutral body were selected as the most promising type of cooling curve for this investigation. A niobium neutral body was placed adjacent to the alloy specimen and both were heated or cooled at such a rate that the temperature difference between them was essentially constant. When the specimen underwent a transformation, a sharp discontinuity was caused in the temperature difference curve. The difference in temperature between the specimen and the niobium neutral body was recorded on the X_2 scale, -1.5 to +1.5 millivolt range, of a Leeds and Northrup Speedomax X-X recorder while the temperature of the specimen was recorded on the X_1 scale, 0 to 20 millivolts, of the same instrument. A small potentiometer, having an output of 0 to 7 millivolts, was connected in series with the differential thermocouple to allow the millivoltage difference between the specimen and the neutral body to be adjusted to zero at the start of the cooling period. This was necessary to prevent the curve from running off scale during the experiments. Thermal effects of much less than 1°C. were easily detected using this method and equipment.

The samples were heated in a molybdenum, tantalum, or niobium wire wound resistance furnace or by induction heating. The resistance furnace core presented a problem since the more common refractories

cannot be used at temperatures up to 1600°C. Cores made of beryllium oxide, which was grooved for the resistance wire, proved to be the most satisfactory. The grooves could be readily cut in the surface of the beryllia by wetting the beryllia with water before grinding. Furnaces constructed using niobium wire seemed to last longer than those made of tantalum or molybdenum. Figure 3 is a drawing of the furnace used to obtain much of the cooling curve data. Essentially the apparatus consisted of the thermocouples (D), a resistance wire winding (E) on a beryllia core (C), a 60 mesh porous graphite insulating sleeve (B), a beryllia or thoria crucible (F) containing the specimen, and a beryllia tube (G) supporting the neutral body and the specimen crucible assembly. This entire unit was supported on a stainless steel tripod (H) within a watercooled copper vacuum chamber (A). The thermocouples were brought out of the top or bottom of the vacuum chamber through small glass-to-metal seals. The electrical leads were brought into the system through a rubber gasket seal (I). Temperatures as high as 1600°C. were obtained in this furnace.

A similar setup was employed when induction heating was used. The essential differences were that the furnace core was replaced by a graphite heater, and the copper vacuum chamber was replaced by a quartz tube. In both cases the vacuum system consisted of a cold trap filled with liquid nitrogen, a large diffusion pump, and a mechanical pump of sufficient capacity to handle the load. Vacuums of the order of 5×10^{-6} to 1×10^{-4} millimeters of mercury were maintained during these experiments.

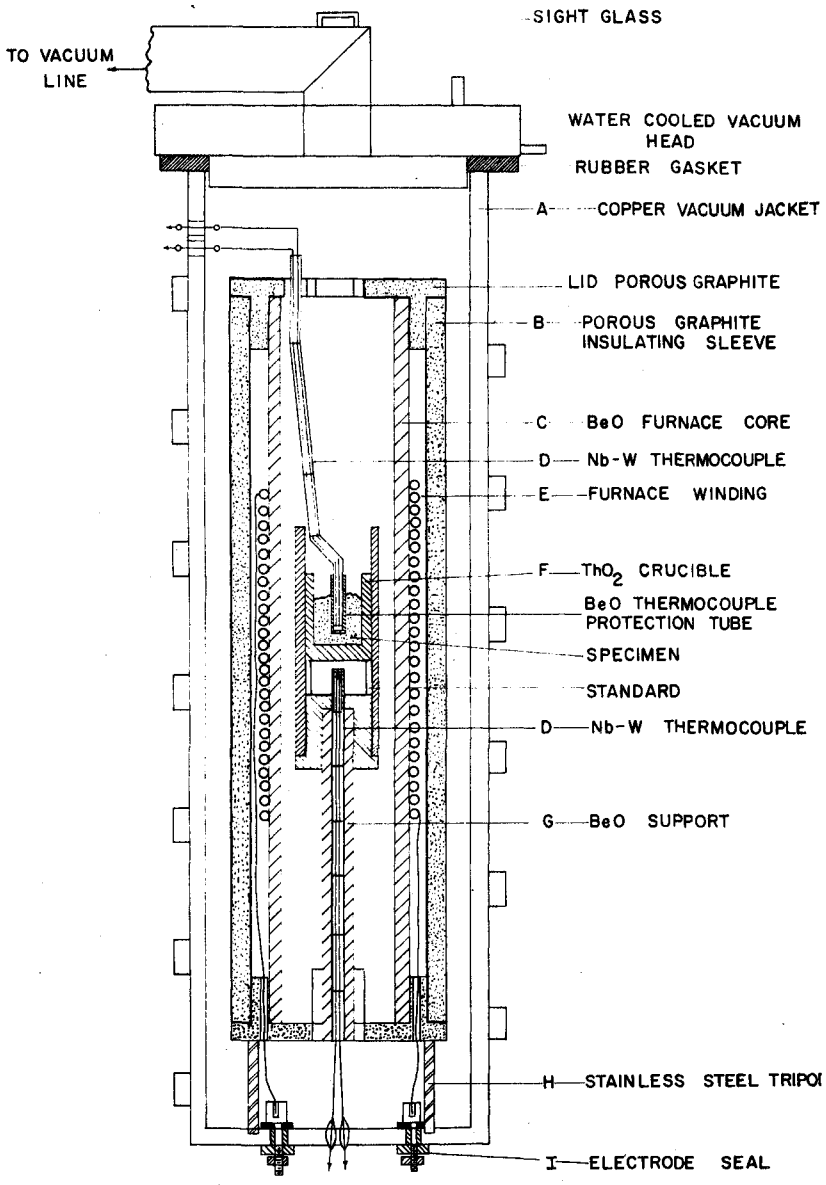

Fig. 3 Cooling Curve Furnace.

A few cooling curves were obtained using a platinum-platinum, 13 per cent rhodium thermocouple. The tube furnace described in conjunction with the determination of the liquidus (section II-B-5) was used to heat the samples.

(b) Melting bar method. Melting points were obtained on a number of alloys using the method described by Pirani and Alterthum (28). Essentially the method consisted of heating a bar of metal by passing a high electrical current through it while observing the melting temperature with an optical pyrometer focused on a small hole that had been drilled in the bar. The melting bars used in this investigation were sections cut from arc melted alloy buttons and measured approximately 1/4 X 1/4 X 2 inches. A hole, 0.31 inches in diameter and over 0.15 inches deep, was drilled normal to the long axis of the bar. The bar was notched by grinding to insure that the melting would first occur in the region of the hole. Temperature readings were taken with a Leeds and Northrup disappearing type optical pyrometer by sighting through a pyrex window in the melting chamber. A temperature correction was made for absorption by the sightglass using the relationship

$$\frac{1}{T} - \frac{1}{T_a} = 0.0000046 \qquad (12)$$

developed by Foote (29) where T_a is the apparent temperature and T is the true temperature in degrees Centigrade.

The temperature at which liquid first appeared was taken as an indication of the solidus temperature. Occasionally a film of oxide

or nitride was formed around the hole preventing the hole from filling with metal. In these cases, since the hole still acted as a black body, the sample was heated until it melted in two, thus giving an indication of the liquidus temperature. Even when the hole did not fill with metal there was often an abrupt change, usually a darkening of the bottom of the hole, that indicated melting had started.

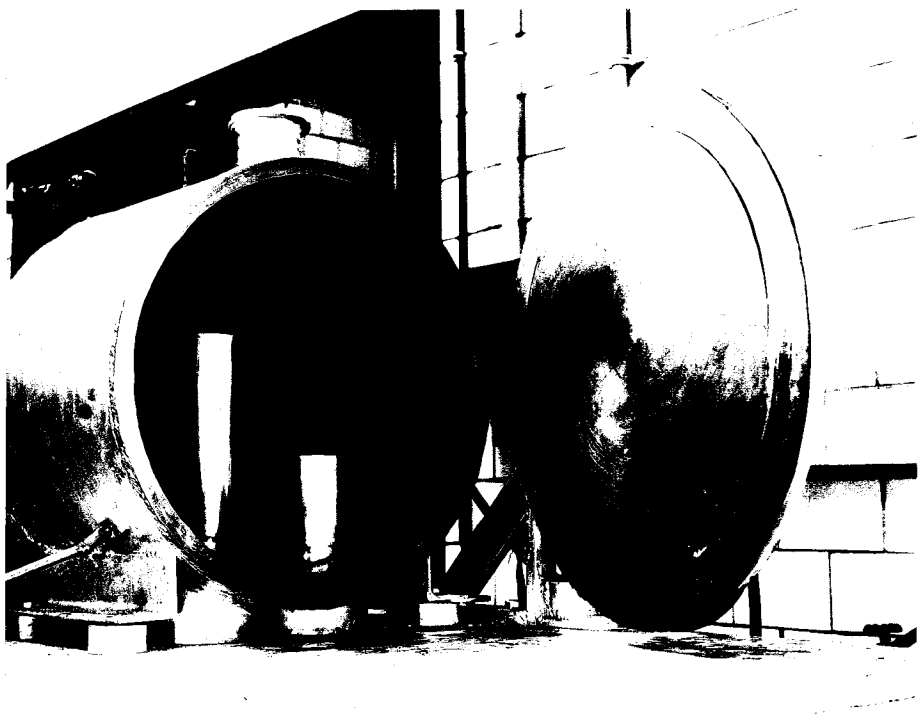

Fig. 4 Vacuum Chamber of Melting Bar Furnace

The apparatus illustrated in Figure 4 was used for these experiments. The furnace consisted of a large water-jacketed vacuum chamber containing two heavy watercooled copper electrodes. The specimen was clamped between a pair of copper bars (Figure 5) that were clamped to the electrodes. A hinged watercooled door was provided to allow easy access to the melting chamber. To seal the vacuum chamber a

rubber gasket was placed between the door and the machined edge of the vacuum chamber, and the door was closed.

A vacuum ranging from 5×10^{-6} to 6×10^{-5} millimeters of mercury was maintained at all times during the melting temperature determinations. The vacuum system was constructed of 6 inch diameter iron

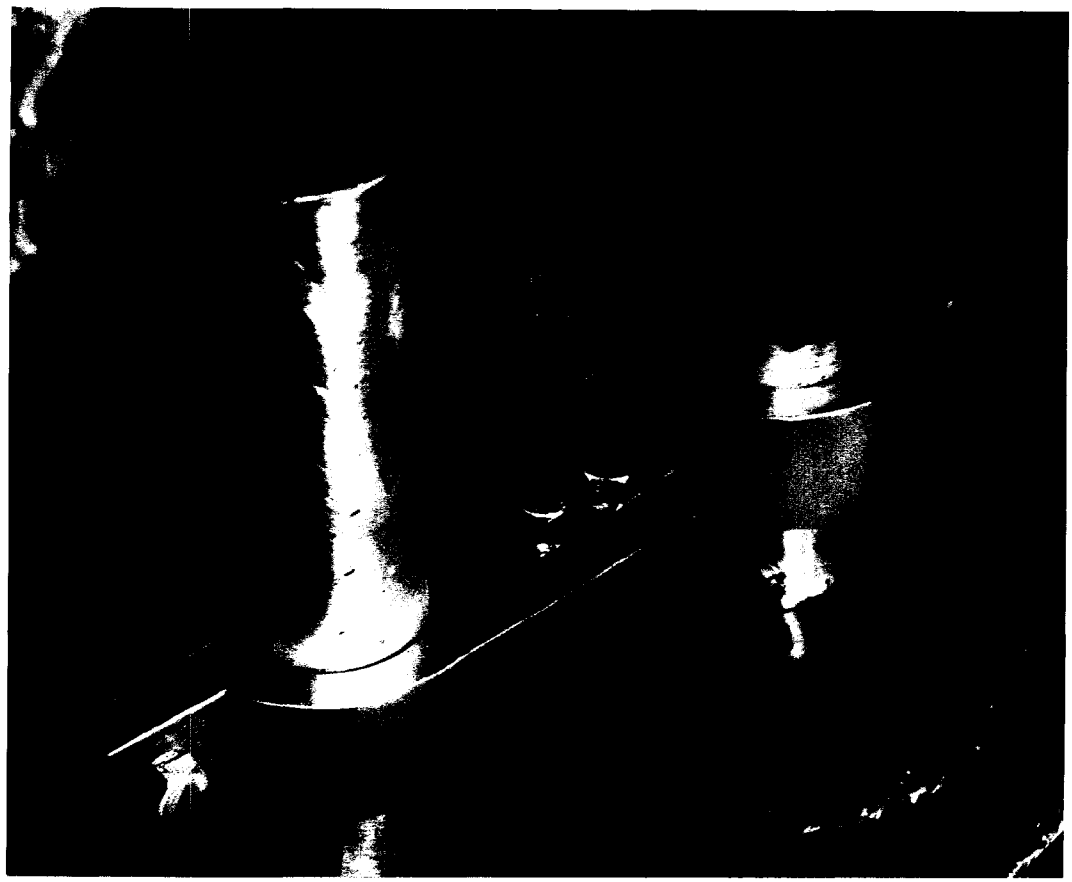

Fig. 5 Melting Bar Clamps in Place

pipe and included a cold trap filled with liquid nitrogen. A large diffusion pump backed by a Kinney mechanical pump provided ample capacity to allow rapid heating to the melting temperature range without losing the vacuum.

Power for this high current furnace was supplied by a 10 KVA.

watercooled step down transformer obtained from the Banner Manufacturing Company. The secondary of this transformer was tapped at 8, 10, and 12 volts and the desired voltage range could be selected with a heavy duty switch. The fine adjustment of the power to the furnace was made by adjusting a two ganged, 53 ampere, 220 volt variac to the desired setting.

(c) Resistance measurements. Resistivity measurements were made on several alloys in the high thorium region of the alloy system using the method and equipment described by Chiotti (30). Essentially the equipment consisted of a furnace much like the one shown in Figure 4. Two additional small electrodes were necessary to allow measurement of the potential drop across the center section of the specimen. Data were recorded directly in ohms on a specially adapted Brown Elektronic recorder.

Alloys were prepared for resistance measurements by swaging arc melted bars into rods approximately 1/4 inch in diameter and 4 inches long. The bars cracked slightly during the swaging process, but in most cases it was possible to select a section of the required length containing very few cracks. The center section of the bar was turned down a few thousandths of an inch to insure that it would be the hottest section of the bar. Small holes were drilled for the tungsten probes, and a hole was drilled to provide black body conditions for optical pyrometer temperature measurements.

5. Liquidus determinations

The thorium rich side of the liquidus curve was determined by measuring the solubility of niobium in thorium at high temperatures. Cylinders of thorium, 1 inch in diameter and 1 inch high, were prepared by arc melting, and a hole 21/64 of an inch in diameter and 11/64 of an inch deep was drilled into the crucible using a lathe. It is important to use a lathe rather than a drill press, as the sample for chemical analysis must be taken from the same hole by drilling and must not include any of the thorium crucible. Bars of a 7.7 per cent niobium-thorium alloy, prepared by arc melting, were swaged into rods and driven into the thorium crucibles. The thorium crucible was then placed in a beryllia crucible and the assembly put in a tantalum tube furnace.

The tantalum tube furnace, illustrated in Figure 6, was connected to the electrodes of the vacuum chamber used for the melting bar experiments with a set of heavy copper adaptors. One of the adaptors is shown lying in front of the furnace in the photograph. After the apparatus was assembled a beryllia lid with a 1/32 of an inch diameter hole drilled through it was placed over the sample crucible to provide black body conditions for temperature measurements.

The sample was heated as rapidly as possible, while maintaining a vacuum of less than 5×10^{-5} millimeters of mercury, to the desired temperature and held at temperature for thirty minutes. Since no insulation was used in the furnace, the sample cooled quite rapidly

when the power to the furnace was shut off at the end of the heating period. Samples were obtained for chemical analyses by drilling two or three concentric holes into the region that had been liquid.

Fig. 6 High Temperature Tube Furnace

6. Chemical analysis

The chemical analyses of the niobium-thorium alloys were performed by the analytical section. The separation of niobium from thorium was based upon the insolubility of niobium in concentrated nitric acid containing sodium fluosilicate. Since niobium was

insoluble in this solution, the residue remaining after the thorium had dissolved was collected on a filter paper, ignited to niobium pentoxide, and weighed. Thorium was determined by precipitating thorium oxalate from the filtrate at a pH of one by adding oxalic acid, filtering, igniting the thorium oxalate to thorium dioxide, and weighing.

C. Presentation and Interpretation of the Data

On the basis of data obtained by microscopic examinations, thermal analyses, resistance measurements, and X-ray diffraction studies, the phase diagram shown in Figure 7 has been proposed for the niobium-thorium alloy system.

1. Classification of the alloy system

Since the niobium-thorium alloy system was expected to be a eutectic system, with the possibility that intermediate phases might be formed, the first experimental studies were designed to either confirm or to disprove this prediction.

(a) X-ray evidence. X-rays provide the most positive and one of the simplest ways to determine the phases in an alloy; therefore, X-ray diffraction patterns were taken of thorium, niobium, and a 52.2 per cent niobium alloy. The phases present in each of these specimens as determined by X-ray methods are listed in Table 3.

Since the predominant phases in this 52.2 per cent niobium alloy

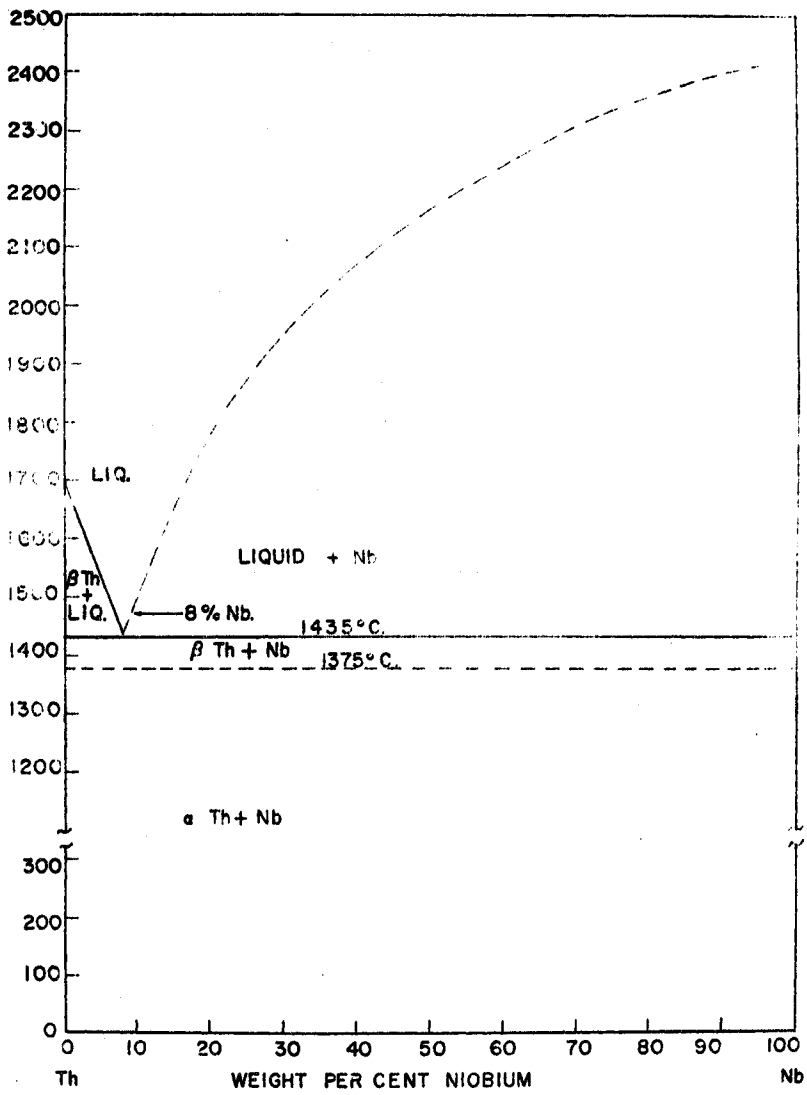

Fig. 7 Niobium-Thorium Phase Diagram.

correspond to niobium and thorium, it appears likely that no stable intermediate phases are present in the niobium-thorium alloy system. Therefore, the alloy system should belong to the immiscible liquid, to the eutectic, or to the eutectic with terminal solid solubility classification.

Table 3. Phase Identification from X-ray Data

Specimen	Phase	Lattice constant A°.	Intensity
Arc melted thorium			
	Thorium	5.089	Strong
	Thorium dioxide		Weak
	A few unidentified lines		Very weak
Arc melted niobium powder			
	Niobium	3.301	Strong
	Niobium carbide or nitride		Very weak
	A few unidentified lines		Very very weak
Arc melted 52.2% niobium alloy			
	Niobium	3.301	Strong
	Thorium	5.087	Strong
	Thorium dioxide		Very weak
	1 unidentified line[a]		Very very weak

[a]The unidentified line found in the X-ray diffraction pattern of the 52.2 per cent niobium alloy corresponds to one of the unidentified lines found in the pattern of the thorium.

(b) Metallographic evidence. Since, on the basis of the predictions discussed in the introduction, it was believed that a eutectic was formed in the niobium-thorium alloy system, the 52.2 per cent

niobium alloy was microscopically examined. The arc melted alloy (Figure 8) contains dendrites of niobium and a fine eutectic structure. After undergoing an annealing treatment at 1285°C. for 2 hours, the same alloy (Figure 9) was unchanged in appearance except for a slight coarsening of the eutectic structure.

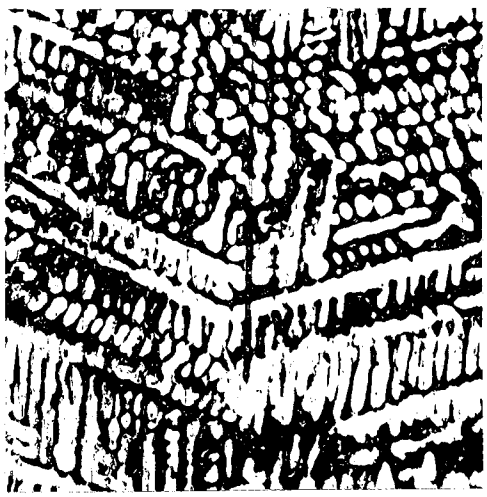

Fig. 8 52.2% Niobium. (As arc melted. White areas are niobium, dark areas are eutectic. Electrolytic etch.[a] X250).

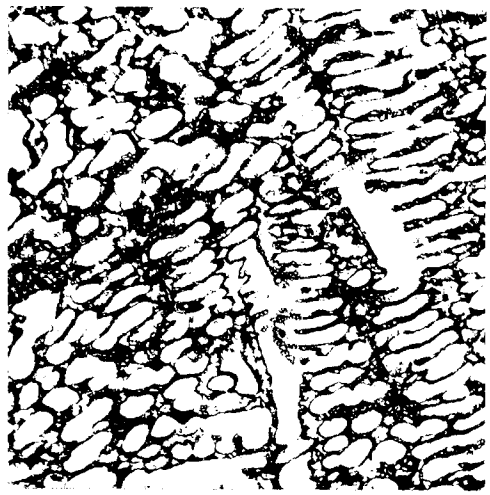

Fig. 9 52.2% Niobium. (Annealed 2 hours at 1385°C. Eutectic slightly coarsened. Electrolytic etch. X250).

Microscopic examination of several niobium-thorium alloys, that had been melted in the melting bar furnace, furnished further evidence that niobium and thorium do not form intermediate phases of any type. Since the ends of the melting bar were in contact with a watercooled electrode clamp while the center of the bar was molten, a large temperature gradient existed between the center and the ends of the bar.

---

[a]All electrolytically etched niobium-thorium alloys were etched in a electrolyte of 3 normal nitric acid containing 1 per cent potassium fluoride.

When the bar melted in half, it cooled very rapidly and was essentially quenched. Therefore, the microstructure along the bar should be representative of alloys quenched from varying temperatures up to the melting point of the bar.

Figures 10, 11, 12, and 13 are photomicrographs of a 3.9 per cent niobium melting bar that had been melted in half. The area of the melting bar that was not heated in this treatment i.e., that was in contact with the clamp, contains a very fine eutectic structure (Figure 10) that was not resolvable at 250 diameters magnification and crystals of primary thorium (the white areas). Figure 11 shows the area of the bar a short distance from the clamp. The eutectic has started to spheroidize slightly. Near the area of the bar that had been molten the spheroidization of the eutectic (Figure 12) was essentially complete. The area of the bar that had been partially molten contains a very fine eutectic structure (Figure 13) that is typical of niobium-thorium alloys which have been spheroidized and then quenched from above the liquid temperature. The structure of this melting bar was typical of all niobium-thorium alloys that had undergone a similar treatment.

A number of niobium-thorium alloys were annealed for varying periods of time (2 to 300 hours) at 1050, 1100, 1285, and 1350°C. and either furnace cooled or quenched. The microstructures of these alloys were very similar to the microstructures of the melting-bars that had been melted. A 5.8 per cent niobium alloy that had been annealed 300 hours at 1100°C. and 2 hours at 1285°C. was heated to 1350°C., held

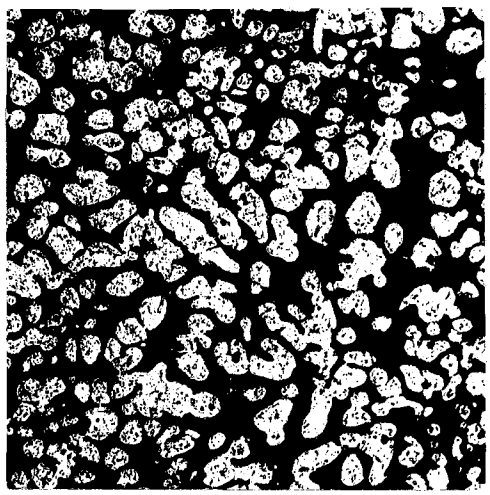

Fig. 10 3.9% Niobium. (Cold end of melting bar. Thorium (white crystals plus fine eutectic. Electrolytic etch. X250).

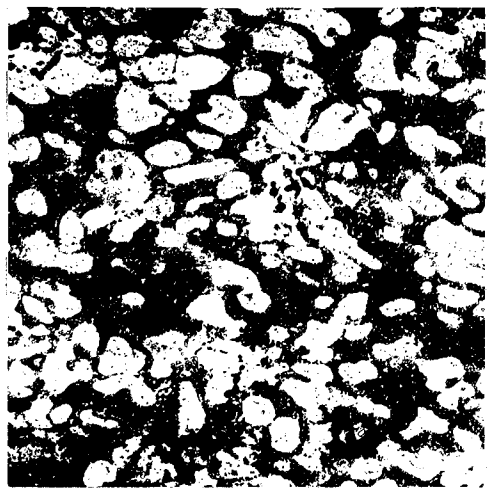

Fig. 11 3.9% Niobium (Near cold end of melting bar. Partially spheroidized eutectic plus thorium. Electrolytic etch. X250).

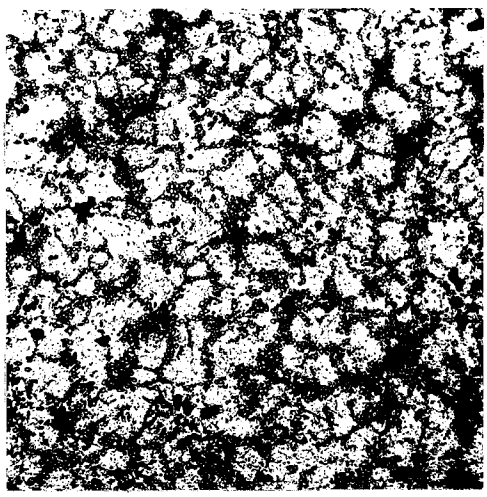

Fig. 12 3.9% Niobium. (Near molten end of melting bar. Spheroidized eutectic plus thorium. Electrolytic etch. X250).

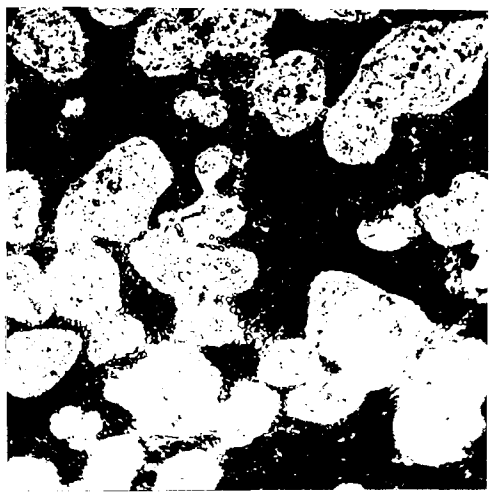

Fig. 13 3.9% Niobium (Partially molten area of melting bar. Thorium plus fine eutectic and some spheroidized niobium. Electrolytic etch. X250).

there a few minutes, and quenched. The structure of this alloy (Figure 14) shows primary thorium (the white areas) and spheroidized eutectic. Figure 15 shows a 6.3 per cent niobium alloy that had been subjected to the 1100 and 1285°C. annealing treatments. Again, the picture shows thorium and spheroidized eutectic. A 9.4 per cent niobium alloy (Figure 16) that had been annealed at 1100°C. for 300 hours has a structure that is essentially spheroidized eutectic containing a few niobium dendrites (the long white needles). The 25.5 per cent niobium alloy, also annealed at 1100°C., contains niobium dendrites and partially spheroidized eutectic.

The contention that a rather complete story of the behavior of the alloys at various temperatures could be read from the microstructures of the melting-bars is upheld by a comparison of the microstructures of the annealed and quenched alloys (Figures 14, 15, 16, and 17) and the microstructures of the melting-bars (Figures 10, 11, 12, and 13).

Since the evidence obtained from X-ray diffraction patterns and metallographic examination of the alloys was compatible only with a eutectic type system, it has been concluded that niobium and thorium form a eutectic. Furthermore, since the lattice constants of niobium and thorium are essentially unchanged in the 52.2 per cent niobium alloy, only very limited terminal solid solubility is possible.

Once the alloy system had been classified, there remained the problems of locating the eutectic, determining the eutectic temperature, determining the shape of the liquidus curve, checking the extent

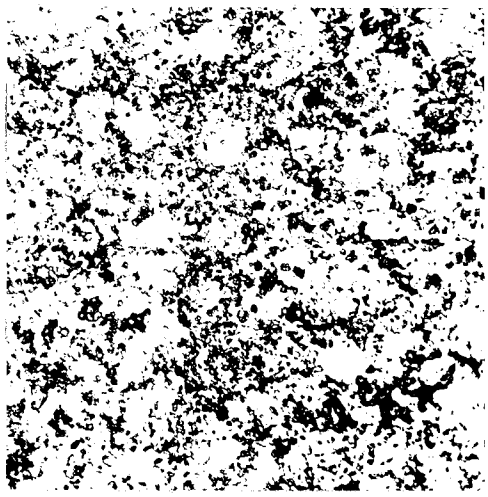

Fig. 14 5.8% Niobium. (Spheroidized, heated to 1350°C., and quenched. Spheriodized eutectic plus thorium. Electrolytic etch. X250).

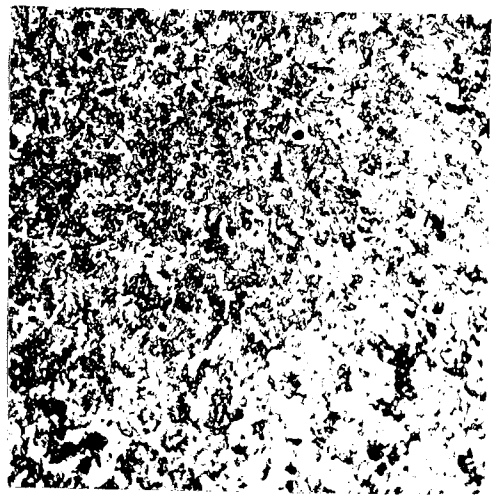

Fig. 15 6.3% Niobium. (Spheroidized at 1285°C. and furnace cooled. Thorium plus spheroidized eutectic. Electrolytic etch. X250).

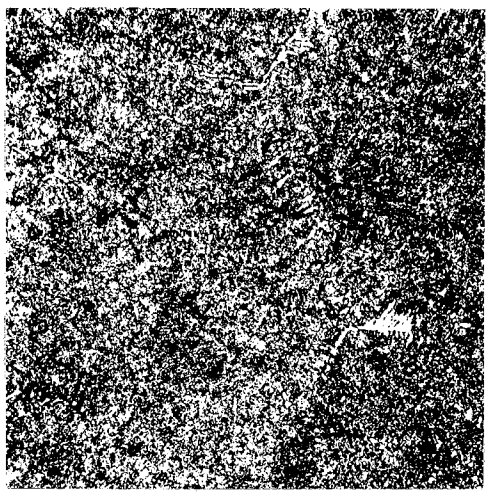

Fig. 16 9.4% Niobium. (Annealed at 1100°C., furnace cooled. Niobium dendrites (white needles) plus spheroidized eutectic. Electrolytic etch. X250).

Fig. 17 25.5% Niobium (Annealed at 1285°C., furnace cooled. Niobium plus eutectic. Electrolytic etch. X250).

of solid solubility, and examining the effect of niobium on the transformation of thorium. These problems are taken up in order in the remainder of this section.

2. Eutectic composition

The eutectic composition, about 8 per cent niobium, was determined primarily by the microscopic examination of niobium-thorium alloys over a wide range of composition. Figure 18 is a photomicrograph of the thorium used in this investigation. The black areas have been identified as thorium dioxide on the basis of previous work and X-ray data. Figures 19, 20, and 21 are photomicrographs of alloys on the thorium rich side of the eutectic. As the niobium content of the alloys increases, the amount of thorium present as primary crystals decreases until at 7.7 per cent niobium (Figure 22) the microstructure is almost completely eutectic. This alloy appears to be just on the thorium side of the eutectic. The 8 per cent niobium alloy (Figure 23) shows an essentially 100 per cent eutectic structure; therefore, 8 per cent niobium is believed to be very near the eutectic composition.

The 9 per cent niobium alloy (Figure 24) is just on the niobium side of the eutectic. Two small dendrites of niobium surrounded by spheroidized eutectic are visible in the photomicrograph. The 12.6 per cent niobium alloy (Figure 25) contains several dendrites of niobium in a matrix of partially spheroidized eutectic. Figures 26, 27, 28, and 29 are photomicrographs of alloys of progressively

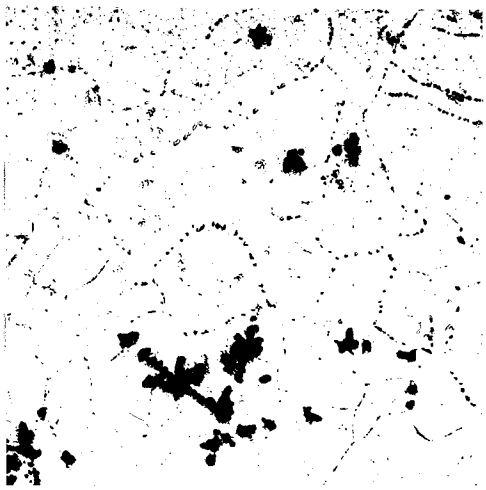

Fig. 18 Thorium. (As arc melted. Black areas are thorium dioxide. Unetched. X250).

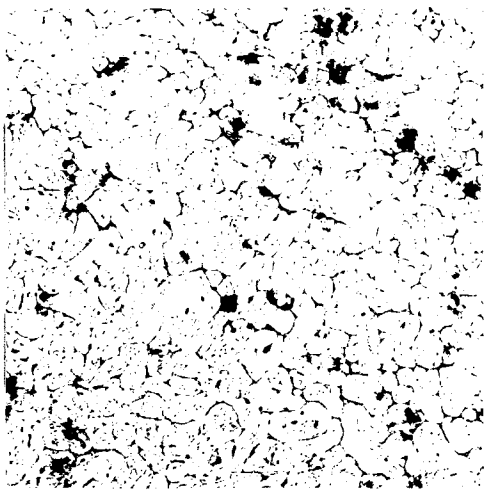

Fig. 19 1.4% Niobium. (As arc melted. Eutectic in grain boundaries. Electrolytic etch. X250).

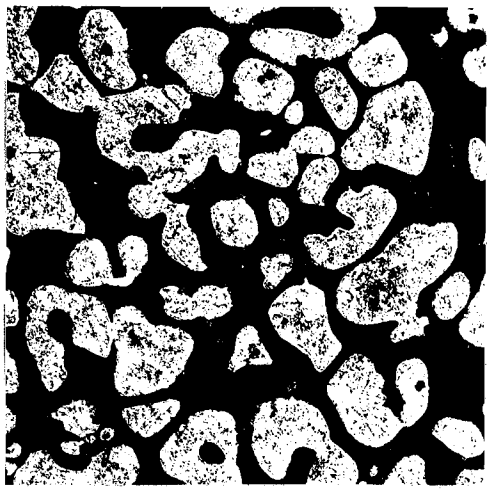

Fig. 20 3.9% Niobium. (Rapidly cooled from liquid state. Thorium (white) plus eutectic. Electrolytic etch. X250).

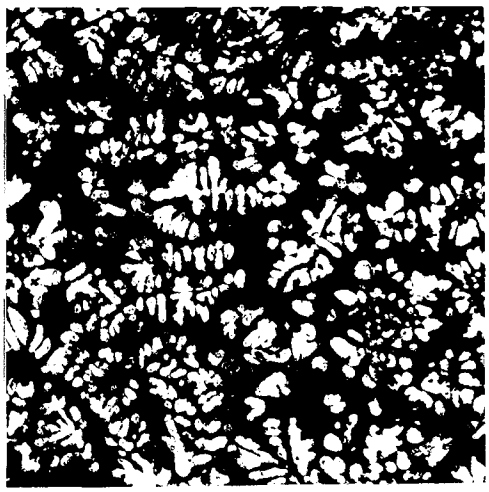

Fig. 21 5.8% Niobium. (As arc melted. Thorium plus eutectic. Electrolytic etch. X250).

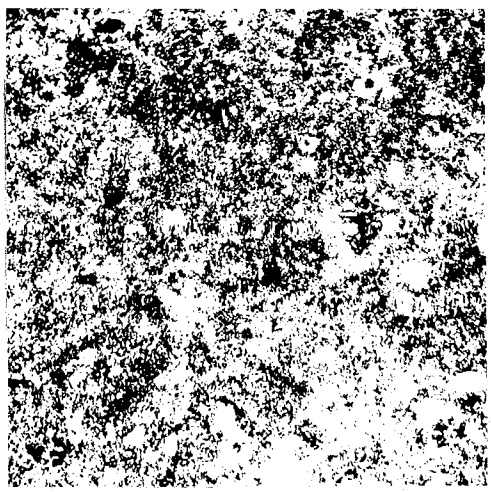

Fig. 22 7.7% Niobium. (As arc melted. Nearly all eutectic. Electrolytic etch. X500).

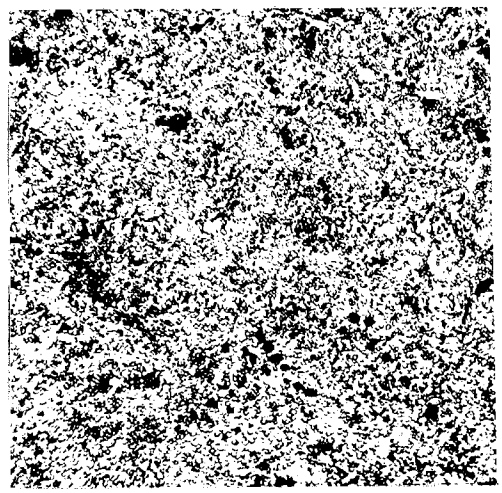

Fig. 23 8.0% (Annealed 8 hours at 1100°C. Essentially all eutectic. Electrolytic etch. X500).

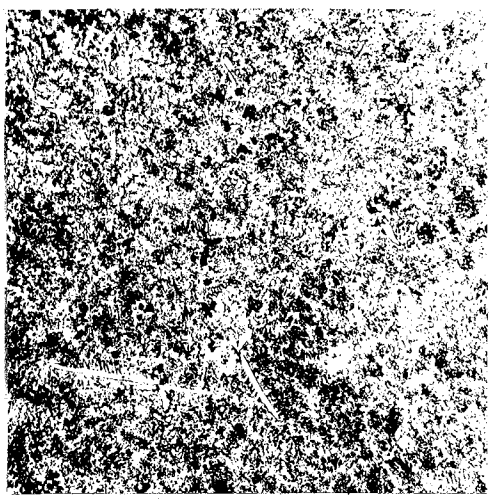

Fig. 24 9.0% Niobium. (Annealed in melting bar furnace. Niobium (white needles) plus spheroidized eutectic. Electrolytic etch. X250).

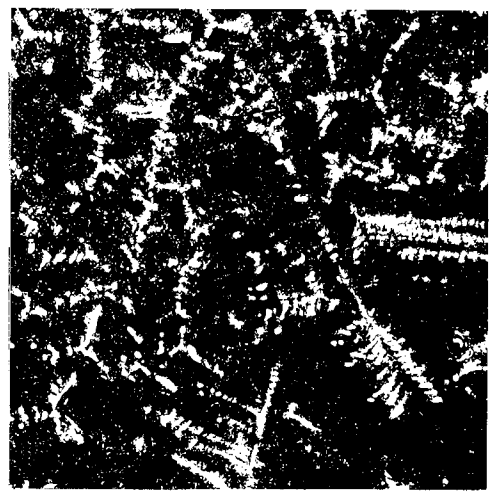

Fig. 25 12.6% Niobium. (Annealed in melting bar furnace. Niobium dendrites plus partially spheroidized eutectic. Electrolytic etch. X250).

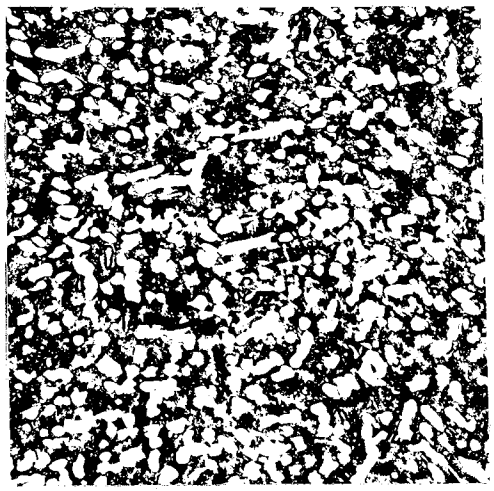

Fig. 26 25.5% Niobium. (As arc melted. Niobium dendrites plus eutectic. Electrolytic etch. X100).

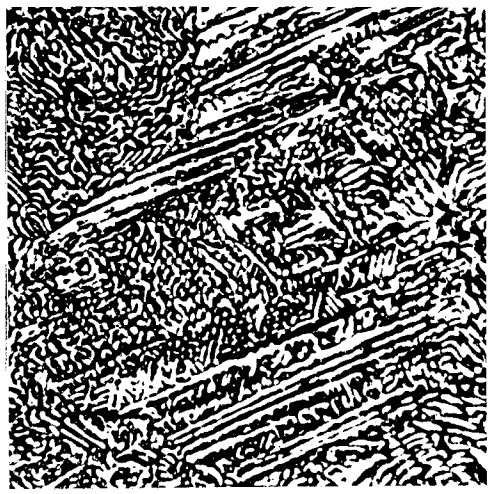

Fig. 27 59.8% Niobium. (As arc melted. Niobium dendrites plus eutectic. Electrolytic etch. X100).

Fig. 28 72% Niobium. (As arc melted. Niobium dendrites and eutectic. Electrolytic etch. X100).

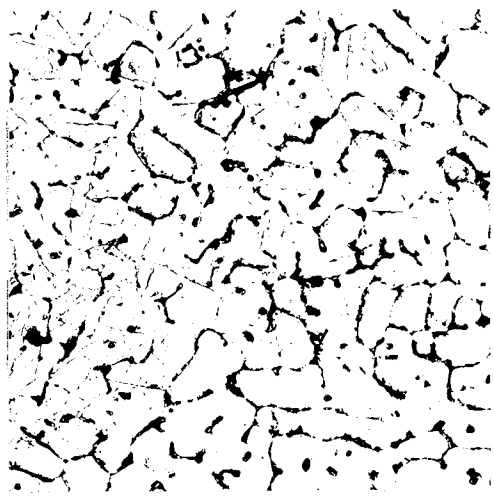

Fig. 29 95% Niobium. (As arc melted. Niobium crystals plus eutectic in grain boundaries. Aqua regia plus 5% HF etch. X250).

increasing niobium content. All of the alloys contain niobium dendrites plus eutectic. The eutectic structure is masked by the impurities in the 99 per cent niobium alloy (Figure 30). Since the eutectic is about 8 per cent niobium, the ratio of eutectic to niobium

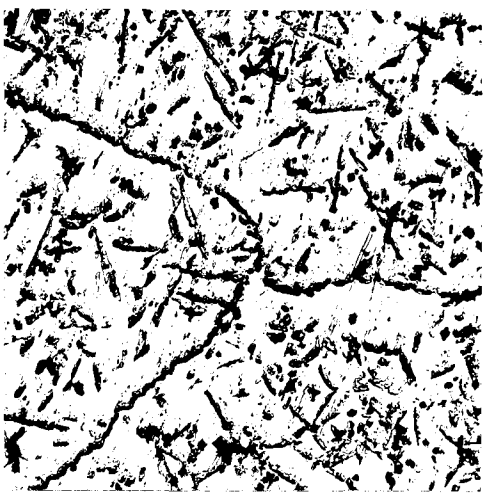

Fig. 30 99% Niobium. (As arc melted. Eutectic on the grain boundaries is masked by impurities. Aqua regia plus 5% HF etch. X250).

Fig. 31 Niobium. (As arc melted. Grain boundary material and needles are impurities. Aqua regia plus 5% HF etch. X250).

dendrites in the 99 per cent niobium alloy should be about one to ninety assuming no solid solubility. Therefore, in view of the large amount of impurities in the niobium metal (Figure 31) it is impossible to definitely identify eutectic structure in the 99 per cent niobium alloy.

As will be shown later, further evidence that the eutectic composition is about 8 per cent niobium was obtained by extrapolating the experimentally determined liquidus curve to the eutectic horizontal.

3. Eutectic temperature

Three independent methods were employed to determine the eutectic temperature. On the basis of the data obtained from thermal analyses, melting temperature determinations, and resistance measurements, the eutectic temperature has been placed at 1435°C. These data are plotted in Figure 32.

(a) Cooling curve methods. The use of cooling curves presented many experimental difficulties which were discussed in the niobium-thorium experimental section (II-B-4) and, as a result, there is some doubt as to the validity of some of the cooling curve data. The cooling curves were obtained with a niobium-tungsten thermocouple using the wire wound resistance furnace or the induction furnace to heat the specimens which were in a beryllia crucible. The cooling curves had a very jagged appearance. This jagged appearance made it very difficult to distinguish the thermal arrests from the remainder of the curve. The jagged appearance of the curves was thought to be due to the pick up of an alternating voltage which was superimposed on the millivoltage of the thermocouple. All attempts at shielding or filtering out this alternating component of voltage met with failure. The breaks in the cooling curves were detected with a niobium-tungsten thermocouple, but the temperature values were read at the time on an optical pyrometer.

A very small thermal arrest occurring in the vicinity of 1350°C. was observed in most of the first series of cooling curves. Since the eutectic temperature reported in the literature was 1315°C. (26), the

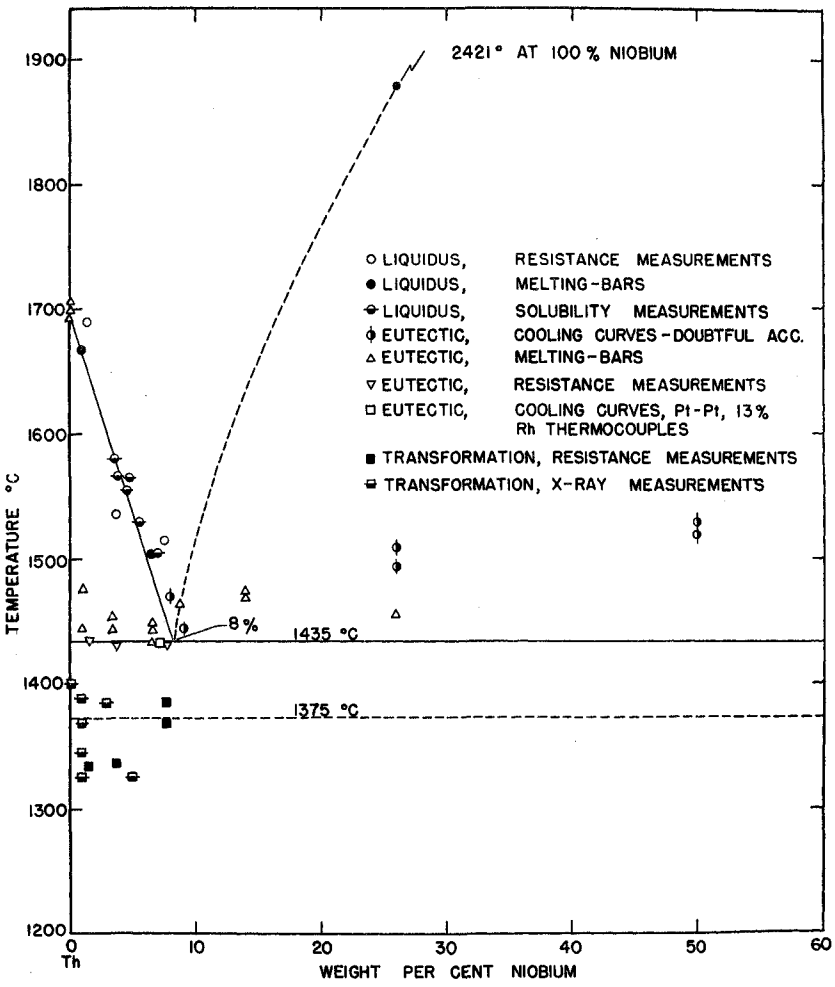

Fig. 32 Thermal, Resistivity, and X-ray Data for the Niobium-Thorium Alloy System.

thermal arrest at 1350°C. was at first thought to be due to the eutectic. However, a close examination of alloys upon which cooling curves had been run failed to reveal any sign of melting even when the alloys had been heated as much as 100°C. above the reported eutectic temperature. A few cooling curves were obtained having a thermal arrest ranging between 1440 and 1535°C. which was attributed to the eutectic. The inherent errors in the method prevented an accurate determination of the eutectic temperature. The significance of the 1350°C. thermal arrest is discussed in conjunction with the effects of niobium on the transformation of thorium (section II-C-6).

Some data were obtained with a platinum-platinum, 13 per cent rhodium thermocouple using the tantalum tube furnace to heat the specimens. Since there was some evidence that a reaction had occurred between the beryllia crucibles and the alloys in the above described experiments, the alloys used in these experiments were melted in thoria crucibles. The results were very satisfactory. Seven separate cooling curves were obtained on a 7.3 per cent niobium alloy and in all seven curves the thermal arrest thought to be due to the eutectic came at 1434 8°C. on both heating and cooling. On the basis of these tests it appears that a value of about 1435°C. for the eutectic temperature represents the best thermocouple data.

(b) Melting bar methods. Melting temperatures were measured on niobium metal, on thorium metal, and on niobium-thorium alloys in the eutectic region using the melting bar method. As a whole the data

obtained by this method were quite consistent. Melting temperatures taken of alloys near the eutectic varied between 1434 and 1465°C. The average value was 1448°C. The average value of all of the melting bar data was 1456°C. Since all of the alloys except the eutectic melt over a range, the values obtained by the melting bar method have a tendency to be high. Table 4 contains a summary of the melting temperatures determined for the niobium-thorium alloy system. The actual value of the eutectic temperature is thought to be slightly less than 1448°C. on the basis of a consideration of the melting bar data.

(c) Resistance methods. Melting temperatures of several alloys on the thorium rich side of the eutectic were determined by measuring the electrical resistivity of the alloys as a function of temperature. Table 5 contains a summary of the breaks in the resistivity versus temperature curves. In all but one case the resistivity curve (a typical curve is shown in Figure 33) passed through a maximum at 1430 to 1435°C. The resistance measurements were made on swaged rods of niobium-thorium alloys, and small cracks were noted in all of the rods except the 5.15 per cent niobium alloy. It is thought that the maximum in the resistance curves is due to the healing of the cracks in the swaged rods. This would effectively increase the cross sectional area of the rods thereby reducing the resistance. Since the alloys were heated quite rapidly, it is possible that the healing of the cracks occurred as the first liquid was formed. This would explain why the maximum occurred at the same temperature in all cases since

Table 4. Melting Temperatures Determined by Melting-bar Method

Alloy composition % Nb	% Th	First appearance of liquid, °C.	Bar melted in two, °C.
1	99	1444 1474 1481	1668
3.6	95.93	1445 1454 1445	
6.64	91.9	1444 ——— 1434 1449	1505
8.97	91.04	1465 1476[a]	
14.07	85.5	1469 1474	
26.39	74.38	1464 1444	1880
0.00	100	1693 1703 1708	
100	0.00	2421	

[a]The bar melted while not being observed.

the first formation of liquid would occur at a constant temperature in a eutectic system. The sharp increase in resistance following the hump in the curve would then be due to the continued formation of liquid metal which has a higher resistance than solid metal.

Table 5. Resistance Curve Discontinuities

Alloy composition		Transformation temperature, °C.	Temperature of the maximum in the curve, °C.	Bar melted in two, °C.
% Nb	% Th			
1.46	95.5	1335	1435	1690
3.7	95.22	1337	1430	1535
5.15	93.24	1287		1415[a]
7.7	92.54	1370	1432	1515
7.7	92.54	1385	1435	1490

[a]Results low, probably due to film on sight glass.

On this basis the eutectic temperature, as determined by electrical resistivity measurements, is between 1430 and 1435°C. This is in good agreement with the value (1448°C.) obtained using the melting bar method and is in excellent agreement with the temperature (1434°C.) obtained by the cooling curve method employing a platinum-platinum, 13 per cent rhodium thermocouple.

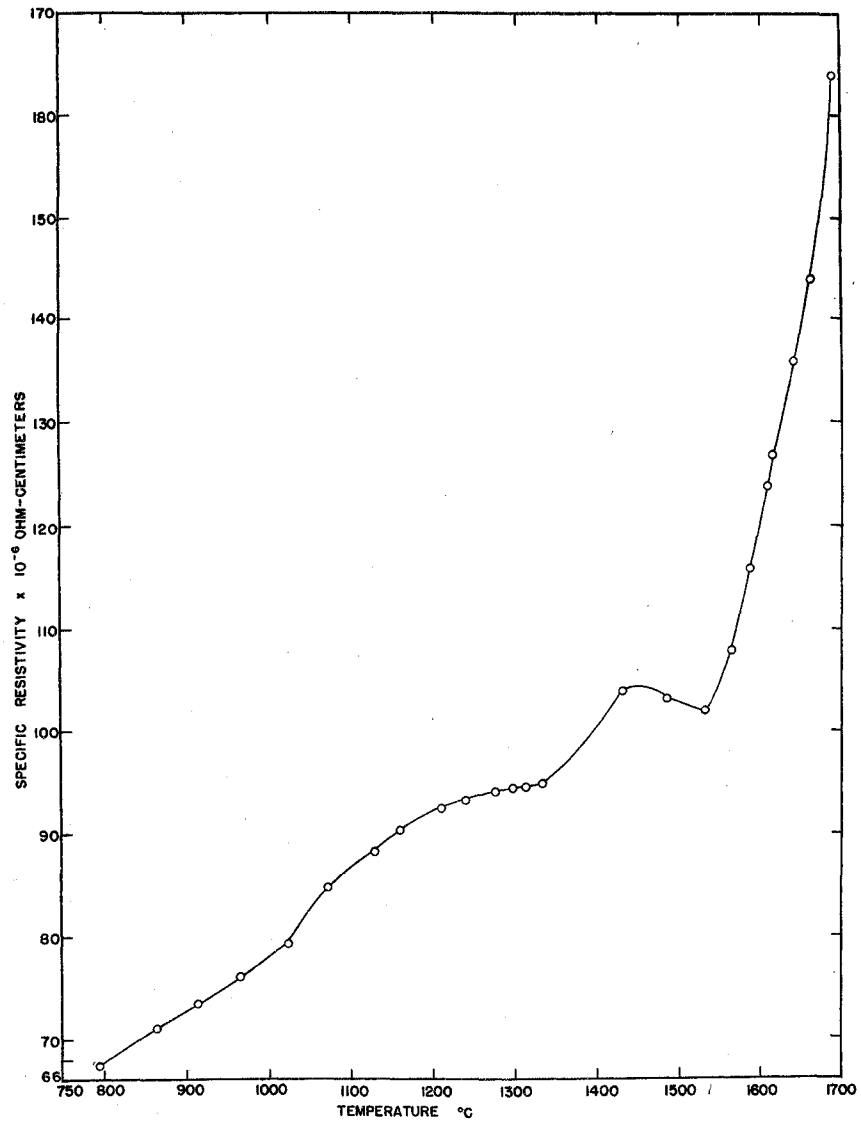

Fig. 33 Typical Resistivity Curve.

4. Liquidus curve

The liquidus curve on the thorium side of the eutectic was determined primarily from data obtained by high temperature solubility studies. The composition, as determined by chemical analysis, of the liquid phases that were in equilibrium with solid thorium at temperatures ranging from 1500 to above 1625°C. are given in Table 6 and shown graphically in Figure 32.

Table 6. Liquidus Compositions

Temperature, °C	Analytical composition					
	Rim		Middle		Core	
	% Nb	% Th	% Nb	% Th	% Nb	% Th
1505	6.78	87	6.94	90.95	7.01	91.18
1530	5.32	95.18	5.46	90.75	5.47	92.1
1555	4.47	94.59			4.23	93.55
1565	4.71	93.42			3.88	94.65
1580	3.58	93.42			3.37	93.95
1625[a]	1.56	99.37				

[a]The entire sample melted during the study at 1625°C. and a film was formed on the sight glass. As a result both the temperature and composition are in error.

To insure that the liquid was homogeneous, two or three separate samples for chemical analyses were removed by drilling concentric holes into the region of the specimen that had been liquid. In these experi-

ments an alloy of essentially eutectic composition was held at the specified temperature in the molten condition in a thorium crucible.

The data of the above described experiments were supplemented by observations made during the melting bar studies and during the resistivity measurements. When it was possible to measure the temperature of the specimen bar, after the eutectic had been reached, the bars were heated until they fell apart. These temperatures are plotted on Figure 32. These points were expected to be low since, due to the rather large difference between the eutectic temperature and the liquidus temperatures, enough liquid would be present to cause the bar to fall apart before it was completely molten. However, often an oxide film formed around the bar and held it together until it was essentially all liquid. Data of this nature is normally useful only as an indication of the true points on the liquidus curve unless the temperature difference between the solidus and liquidus happens to be small. The plot (Figure 32) shows fairly good agreement between the three different experimental methods. The liquidus has been sketched as a straight line.

The determination of the liquidus curve also furnished further evidence as to the eutectic composition. The point of intersection of the liquidus curve and the eutectic horizontal is in good agreement with the microscopic evidence as to the location of the eutectic point.

5. Terminal solid solubility

The lattice constant of the niobium used in this investigation was found to be 3.301 Angstroms and the lattice constant of the niobium phase of a 52.2 per cent niobium alloy was also found to be 3.301 Angstroms. Since there was no change in the lattice constant, the solid solubility of thorium in niobium should be insignificant.

Since the lattice constant of thorium changed from 5.089 to 5.087 Angstroms upon the addition of 52.2 per cent niobium, there was a possibility that there might be limited solid solubility of niobium in thorium. Eutectic structure could still be recognized in a 1 per cent niobium alloy; therefore, the solubility of niobium in thorium must be less than 1 per cent.

Back-reflection X-ray diffraction patterns were taken of a series of alloys containing less than 1 per cent niobium. A correction was made for film shrinkage using the method outlined in section II-B-3 and the lattice constants were calculated using the method of extrapolation suggested by Nelson and Riley (31). Figure 34 shows a typical extrapolation curve constructed using the data (in this case for thorium) calculated from an X-ray diffraction pattern.

Figure 35 is a plot of the lattice constant of thorium against weight per cent niobium. From this curve it appears that the solubility of niobium in thorium is less than 0.1 per cent. However, small changes in the impurity content of thorium might also be responsible for this small change. It has been shown (21) that carbon increases the lattice

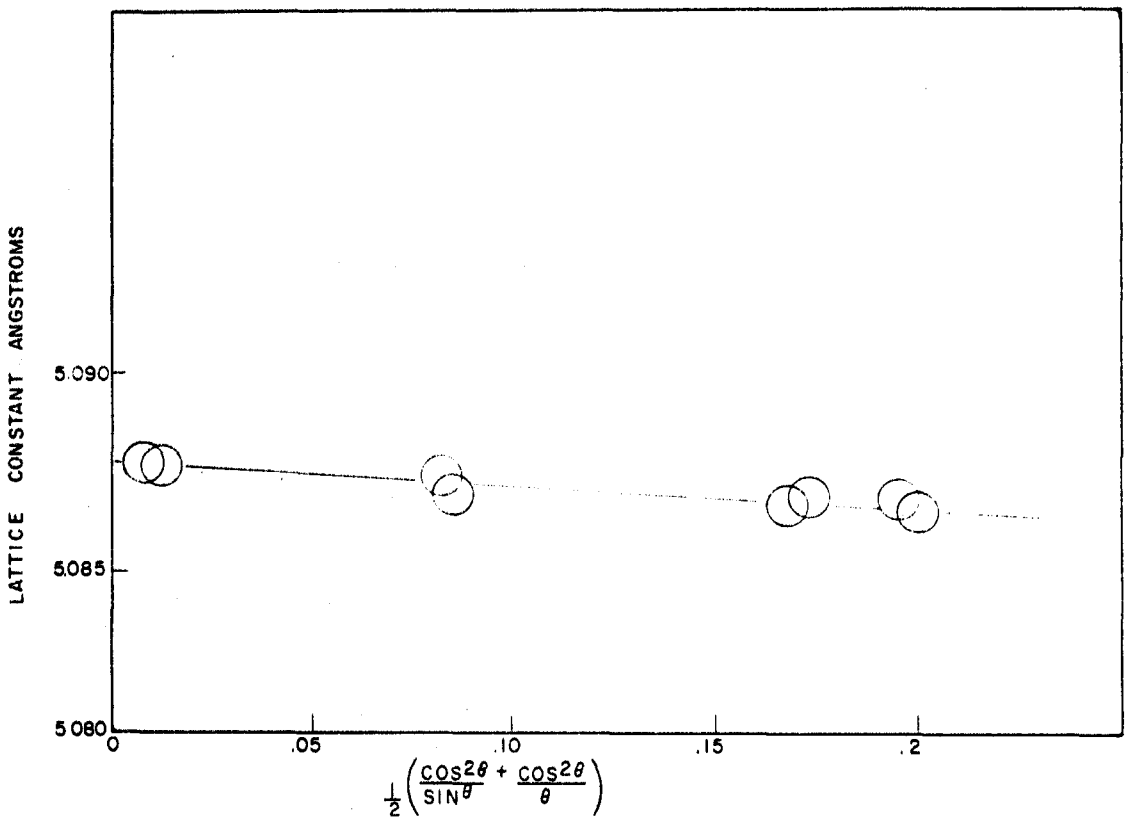

Fig. 34 Typical X-ray Extrapolation Curve Using Nelson and Riley Function.

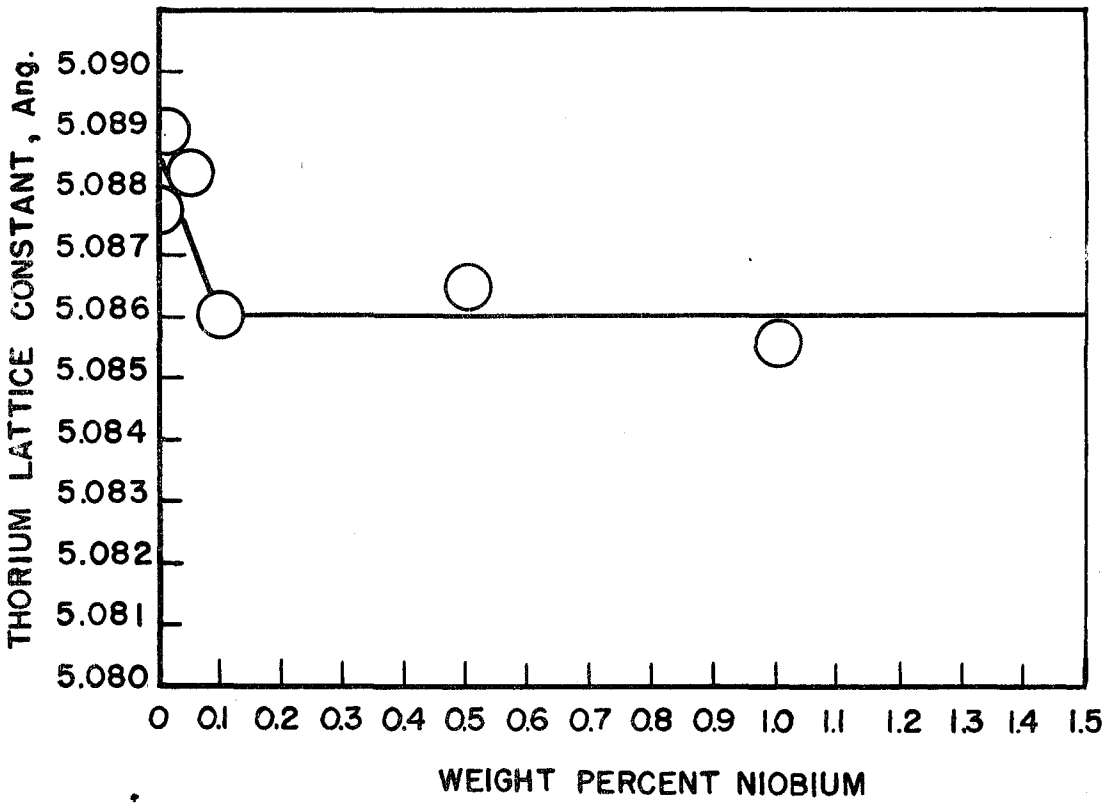

Fig. 35 Change in Lattice Constant of Thorium Upon the Addition of Niobium.

constant of thorium. On the basis that niobium ties up the carbon in thorium, it has been calculated that 0.2 per cent niobium would be necessary to lower the lattice constant of this thorium by 0.002 Angstroms. Since the addition of only 0.1 per cent niobium lowered the lattice constant 0.002 Angstroms, this lowering cannot be completely explained by assuming that it is due to the niobium tying up the carbon that was in the thorium. Therefore, it seems reasonable to believe that there is very limited, less than 0.1 per cent, solid solubility of niobium in thorium at room temperature.

The solubility of niobium in β thorium is thought to be much less than 1 per cent at the eutectic temperature, since a eutectic melting point was observed on the 1 per cent niobium alloy. Eutectic structure was also observed in the grain boundaries of the 1 per cent alloy. The lattice constant of β thorium has been reported as 4.116 Angstroms at 1405°C. The value of the lattice constant of the solid β thorium phase of a 1 per cent niobium alloy was found to be 4.119 at 1455°C. All of these values may be somewhat in error since they are based upon only front reflection peaks. However, since no appreciable change occurred in the lattice constant of β thorium upon the addition of small amounts of niobium, it has been concluded that the solubility of niobium in β thorium is very limited.

6. Effect of niobium on the $\alpha - \beta$ transformation of thorium

Chiotti (22) has recently identified an allotropic form of thorium that exists above 1400 ± 25°C. The high temperature form is body-

centered cubic and has a lattice constant of about 4.116 Angstroms at 1400°C. The effects of impurities on the transformation is only partially known; however, carbon has been shown to raise the transformation temperature drastically. Since the actual temperature at which the transformation occurs in high purity thorium is not accurately known, it is very difficult to establish with any degree of certainty the effects of niobium on the transformation.

Resistivity versus temperature curves were obtained upon several thorium rich alloys and in every case a break that was due to the transformation of thorium was detected. The temperatures at which this break occurred were badly scattered between 1335 and 1386°C. (Table 5). This rather large variation in the transformation temperature was not unexpected since the break starts over a rather large temperature range in thorium. However, the resistivity break observed in the niobium-thorium alloys came at a somewhat lower temperature than that observed for thorium.

During the cooling curve studies employing a niobium-tungsten thermocouple, a small thermal arrest was observed anywhere from 1275 to 1400°C. Once it had been established that this break was not due to the eutectic, it was thought that it was due to the transformation in thorium. Since there was such a serious scattering of temperatures at which the break occurred, several cooling curves were obtained using a platinum-platinum, 13 per cent rhodium thermocouple. In no case was a break that could be attributed to the transformation observed. Consequently, it is thought that the thermal arrests obtained with

niobium-tungsten thermocouples are due to some other factor than the transformation of thorium. It appears that the heat of transformation for the $\alpha - \beta$ transition of thorium is very small. This is not too surprising since the heat of fusion of thorium is known to be very small.

Table 7. High Temperature X-Ray Results

Alloy composition Wt. % Nb	Transformation temperatures			
	Heating		Cooling	
	Started	Finished	Started	Finished
0.1	1370	1415	1355	1335
1	1390	1415	1385	1335
	1345			
	1325	1390	1345	1320
	1375	1370		
3	1385	1405	1370	1355
5[a]	1325	1325		
Th	1400 25			

[a]The furnace shorted out and destroyed the sample during the experiment.

High temperature X-ray data were also obtained on several thorium rich alloys. These data are listed in Table 7. Again, there is a large scattering in the values observed for the transformation temperature. Such a scattering has also been observed for the transformation

in thorium that contains no niobium; in fact, the transformation temperature has been observed from about 1325 to over 1550°C. in thorium with varying minor impurities.

The evidence obtained from both the resistance data and the X-ray data indicate that the addition of niobium to thorium lowers the transformation temperature of thorium slightly. Since there appears to be very limited solid solubility, if any, of niobium in β thorium, this lowering may be due to the effect of niobium on the impurities in thorium. However, since there is some evidence that there may be very limited solid solubility of niobium in β thorium, this lowering might be due to the formation of a eutectoid in the very high thorium region of the phase diagram. Several alloys containing less than 1 per cent niobium were microscopically examined, but no evidence of eutectoid structure was found. Since, even relatively pure thorium contains a considerable amount of a precipitation within the grains, it is difficult to draw a definite conclusion as to the possibility of a eutectoid formation from microscopic evidence.

III. THE NIOBIUM-VANADIUM ALLOY SYSTEM

Niobium-vanadium alloys were investigated with the intention of proposing a phase diagram for the niobium-vanadium alloy system. The workability and corrosion resistance of the alloys were also investigated.

A. Historical

The element vanadium was discovered in an iron ore from Smaland in 1831 by Sefstrom (32). The first fairly pure vanadium metal was produced in 1869 by Roscoe (33) who reduced vanadium dichloride with hydrogen. The principal sources of vanadium are hydrous calcium vanadates and vanadium sulphides, such as those mined at Minasraga, Peru. The main vanadium ores found in this country are roscoelite and carnotite (34).

Vanadium is a hard, corrosion resistant metal that is used extensively in the production of alloy steels. It has an atomic number of 23, an atomic weight of 50.95, and a density of 5.96 grams per cubic centimeter (13). Values of the melting point that have been reported range from 1700 to 1900°C. The correct value is probably near 1860°C. (35). The only reported form of vanadium is body-centered cubic with a lattice constant of 3.039 Angstroms.

A brief description of niobium was presented in section II-A (Historical) in conjunction with the investigation of the niobium-

thorium system. The most commonly accepted values of the physical properties of niobium are as follows:

Melting point	2415°C.
Density	8.57 grams per cubic centimeter
Structure	body-centered cubic, a^{o} = 3.008 Angstroms

A search of both classified and unclassified literature revealed no reports of any investigations of the niobium-vanadium alloy system. Many investigators have reported methods of preparing vanadium metal. McKechnie and Sebolt (36) prepared massive vanadium in a bomb by reducing vanadium pentoxide with calcium using iodine as a temperature booster. Long (37) prepared an extensive survey of the literature on vanadium production.

B. Apparatus and Experimental Methods

Many of the methods and much of the apparatus described in connection with a similar section on the niobium-thorium alloy system (section II-B) were found to be equally applicable to the study of the niobium-vanadium alloy system. Therefore, only the methods, techniques, and apparatus that differ from those described earlier are presented in this section.

1. Preparation of vanadium metal

No source of ductile vanadium was commercially available to the author at the start of this investigation; consequently, it was necessary to prepare all of the vanadium used for this study from high purity vanadium pentoxide. The reduction of vanadium pentoxide to

vanadium metal was made in a sealed iron reaction vessel commonly called a bomb. The bomb was constructed from a 15 inch section of 4 inch diameter pipe by welding an iron plate over one end (the bottom) and a companion flange on the top. A blind flange, made of one-half inch steel plate, served as a lid and could be bolted in place. A spark plug was screwed into a threaded hole near the top of the bomb to serve as an insulated electrical terminal, and a coil of niobium wire was connected between the bomb wall and the center electrode of the spark plug after introducing the charge. A liner of electrically fused dolomitic oxide was jolt packed in the bomb to prevent the occurrence of a reaction between the pipe wall and the charge. The bomb was sealed by inserting a soft copper gasket between the flange on the bomb and the lid. The reaction was initiated by passing an electrical current through the coil of niobium wire. The current was increased slowly by means of a Variac, at a safe distance, until the charge in the neighborhood of the coil was heated to ignition.

The reactants, their sources, their purities, and the amounts used for a charge are listed in Table 8. The dried reactants were weighed rapidly placed in an argon filled mason jar, and then tumbled for a minimum of ten minutes to insure thorough mixing. A stream of argon was played over the reactants while they were being transferred to the bomb. The purpose of using an inert atmosphere was twofold. The air was displaced, thereby reducing the amount of gaseous contamination during the reduction and, perhaps even more important, the reactants were kept dry. A number of explosions have occurred at this labora-

tory while experimentally preparing vanadium in bombs in which the reaction was initiated by external heating. No explosions have yet occurred while preparing vanadium using the method just described in which a hot wire is employed to initiate the reaction.

Table 8. Typical Charge for Vanadium Reduction

Reactants	Source	Purity %	Weight used grams
V_2O_5	Vanadium Corporation of America	99.92	480
I_2	Mallinckrodt	99	240
Ca	Ames Laboratory of the Atomic Energy Commission	99.9	900

Massive, but unevenly shaped biscuits of vanadium were produced in the bombs. The slag remaining on the metal, after a biscuit was taken out of a bomb, was removed by leaching first in water and finally in dilute hydrochloric acid. Yields ranged from 70 to 80 per cent of the theoretical.

After the metal had been cleaned, it was arc melted into 75 to 100 gram buttons, cold rolled into 10 mil sheet, cut into one-half inch squares, and stored in a desiccator until needed for alloy preparation. Very minor amounts of calcium, iron, manganese, silicon, zirconium, chromium, and possibly niobium were detected in the bomb reduced vanadium by qualitative spectrographic analysis.

2. Preparation of alloys

The majority of the alloys of the niobium-vanadium system were prepared, as described earlier for the niobium-thorium alloys, by arc melting together pressed pills of Fansteel niobium powder and the small pieces of sheet vanadium. Several alloys were made from trimmings off niobium sheet and the sheet vanadium. After the alloys had been arc melted they were cut in half on a silicon carbide cut-off wheel. The alloys were extremely difficult to cut, and it often took as long as 50 minutes to make one cut through an alloy disc $\frac{1}{4}$ inch thick by $1\frac{1}{2}$ inch diameter. This was particularly true for alloys containing over 30 per cent of the powdered niobium metal.

3. Determination of approximate melting temperatures

The niobium-vanadium alloys were extremely brittle and could not be cold worked; therefore, to homogenize the alloys it was desirable to anneal the alloys at as high a temperature as possible without melting. This, of course made it necessary to obtain the approximate melting temperatures of several of the alloys.

Very small sections of the alloys were melted in an induction furnace and the melting observed with an optical pyrometer. The melting temperatures determined for these alloys are listed in Table 9. To allow the temperature measurements to be made under black body conditions, the furnace shown in Figure 36 was constructed.

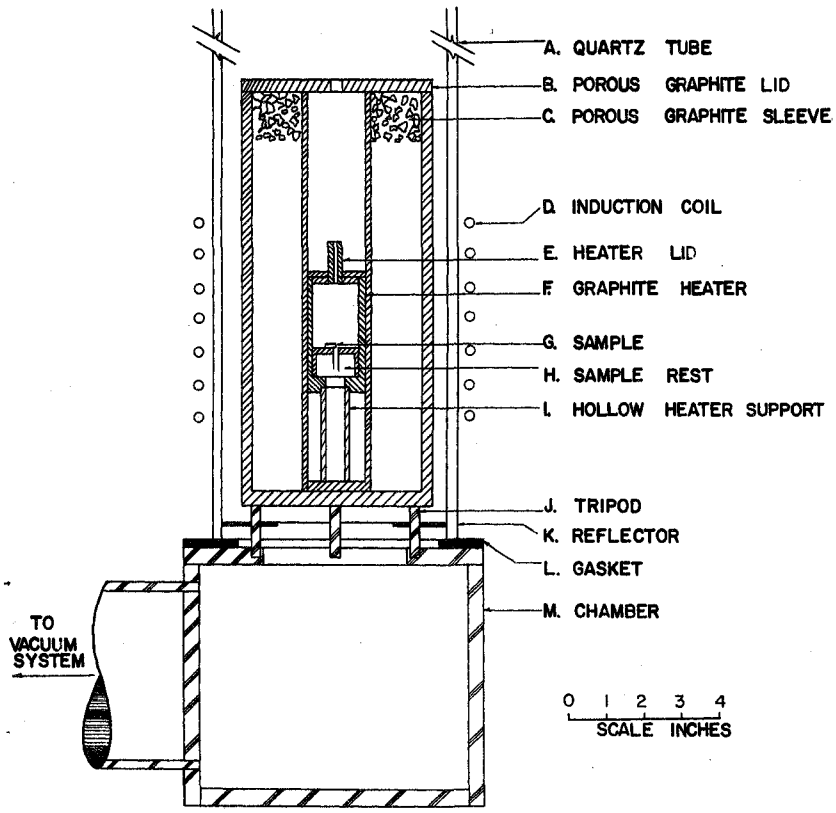

Fig. 36 Approximate Melting Temperature Furnace.

Two concentric porous graphite sleeves (C), which were held in place by porous graphite caps (B) over their ends, were supported on a stainless steel tripod (J) within a quartz tube vacuum chamber (A). The annulus between the porous graphite sleeves was filled

Table 9. Approximate Melting Temperatures of Niobium-Vanadium Alloys

Alloy composition % Nb	Melting temperatures[a] °C.
10	1605
20	1600
40	1602
70	1800

[a]Evidence presented in a later section (III-C-2) will show that these values are considerably low.

with Norblack insulation. A graphite heater (F), which had a one-half inch hole drilled through its bottom, was supported inside the sleeves by a hollow, porous graphite rod (I). A slot was cut through the bottom of a small graphite crucible (H) and the crucible was inverted and placed inside the heater. The sample (G) was then placed on the inverted crucible in such a manner that part of the sample protruded over the slot. Since the bottom of the furnace was several hundred degrees cooler than the sample, the sample could be seen clearly against the black background of the slot. Therefore, by using a lid with a small hole drilled through it, temperatures

could be read with an optical pyrometer under black body conditions while still observing the sample.

Approximate melting temperatures were determined on 10, 20, 40, and 70 per cent niobium-vanadium alloys. The samples were heated slowly by increasing the power output of the high frequency convertor until the sample was visually observed to melt. These temperatures were taken as an indication of the solidus curve of the phase diagram, and were considered to be fairly accurate at the time the approximate melting temperatures were taken.

4. Annealing treatment

After the approximate melting temperatures of the alloys had been determined, one-half of each arc melted specimen was annealed for 4 hours just below the melting temperature. This treatment was designed to homogenize the alloys; however, several of the alloys picked up carbon during the annealing treatment and a eutectic was formed with the carbide impurity. Since this additional carbon content made the study of the alloys very difficult, the remaining half of each alloy was not given this high temperature anneal. A portion of the unannealed half of each of the alloys was later annealed for 48 hours at 1075°C. in a resistance wire furnace.

When the furnace that was used in the approximate melting temperatures and annealing experiments was designed, an attempt was made to make it as versatile as possible. As shown in Figure 36 the heater and insulation has been built as a unit such that it may easily be

replaced if desired. A rather novel watercooled vacuum head (Figure 37) was used to seal the top end of the quartz tube of this equipment. An auxillary sight glass (G) to prevent fogging of the sight glass (C) by metal vapors was hinged to the top of the vacuum head. When the system was under vacuum, the force of the external pressure compressed the copper bellows (E) and the rod extending through the bellows forced the auxillary sight glass against the top of the vacuum head as shown in position (X). When a temperature reading was taken the rod extending through the bellows was pulled, causing the bellows to extend and dropping the auxillary sight glass to position (Y). The auxillary sight glass could be kept in position (Y) by placing one end of the lever (H) against the outside of the vacuum head. Four small glass-to-metal seals (J) were soldered into the vacuum head so that electrical or thermocouple connections could be made in the vacuum system. A needle valve (I) was provided to allow the system to be flushed with an inert gas when desired. The sight glass (C) was held between two "O" rings by a knurled cap (A) that was screwed on to a short section of a pipe welded to the top of the vacuum head.

5. Metallographic examination

It was very difficult to obtain satisfactory metallographic surfaces on the niobium-vanadium alloys. While the alloys were not exceptionally hard, it was necessary to use several sheets of dry grinding paper of each grit size to prepare a good surface on the

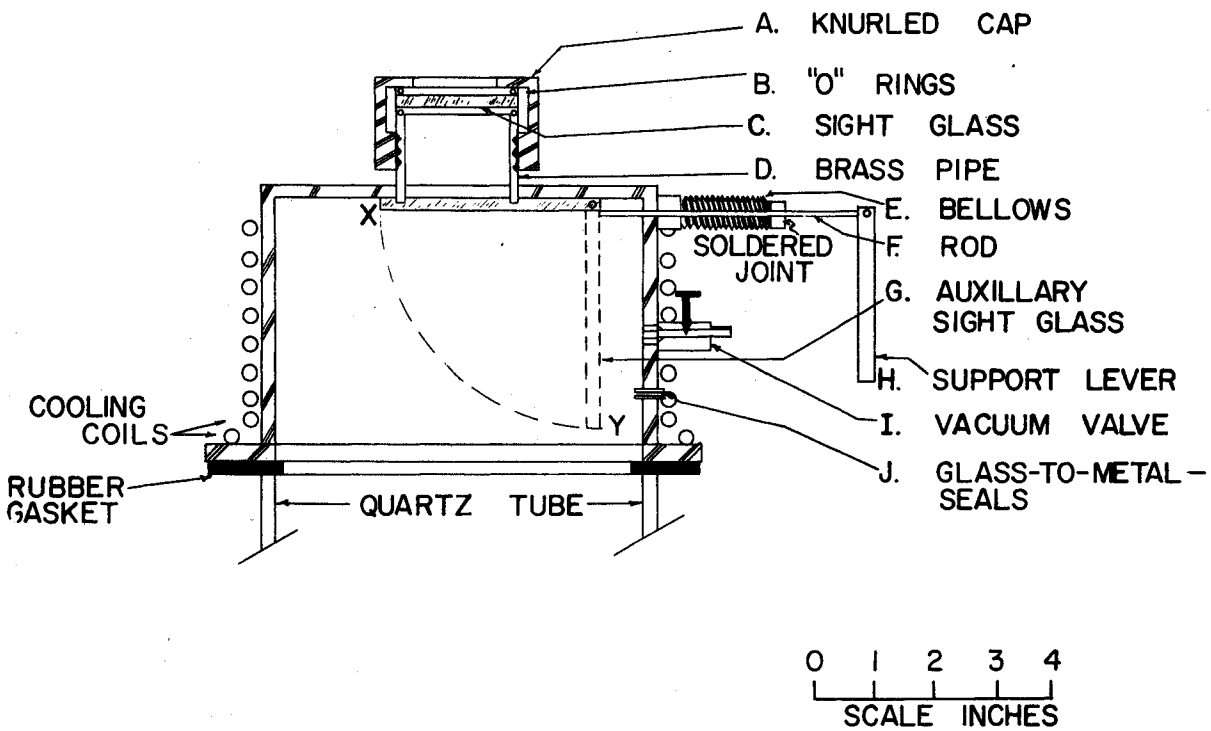

Fig. 37 Vacuum Head.

alloy specimen. To overcome this difficulty, the rough grinding was carried out on a belt grinder using kerosene as a lubricant, and the final grinding operations were done on silicon carbide paper using water as a lubricant. The use of the wet grinding methods produced fairly good surfaces. The alloys were wet polished on a billard cloth covered wheel using as an abrasive a paste made of soap and Linde "A".

Due to the high resistance to chemical attack of niobium-vanadium alloys a considerable amount of difficulty was encountered in trying to etch the specimens. The only satisfactory etching solution found was a mixture of two parts nitric acid, one part sulfuric acid, one part 48 per cent hydrofluoric acid, and one part water. This etchant revealed macro as well as micro structure. All the specimens were etched by immersing them in the etching solution for about thirty seconds.

C. Presentation and Interpretation of the Data

On the basis of evidence obtained by microscopic examination, melting determinations, and X-ray measurements a phase diagram (Figure 38) has been proposed for the niobium-vanadium alloy system. Niobium forms a complete series of solid solutions with vanadium.

1. Classification of the phase diagram

(a) Identification of impurities. Figures 39 and 40 are photo-

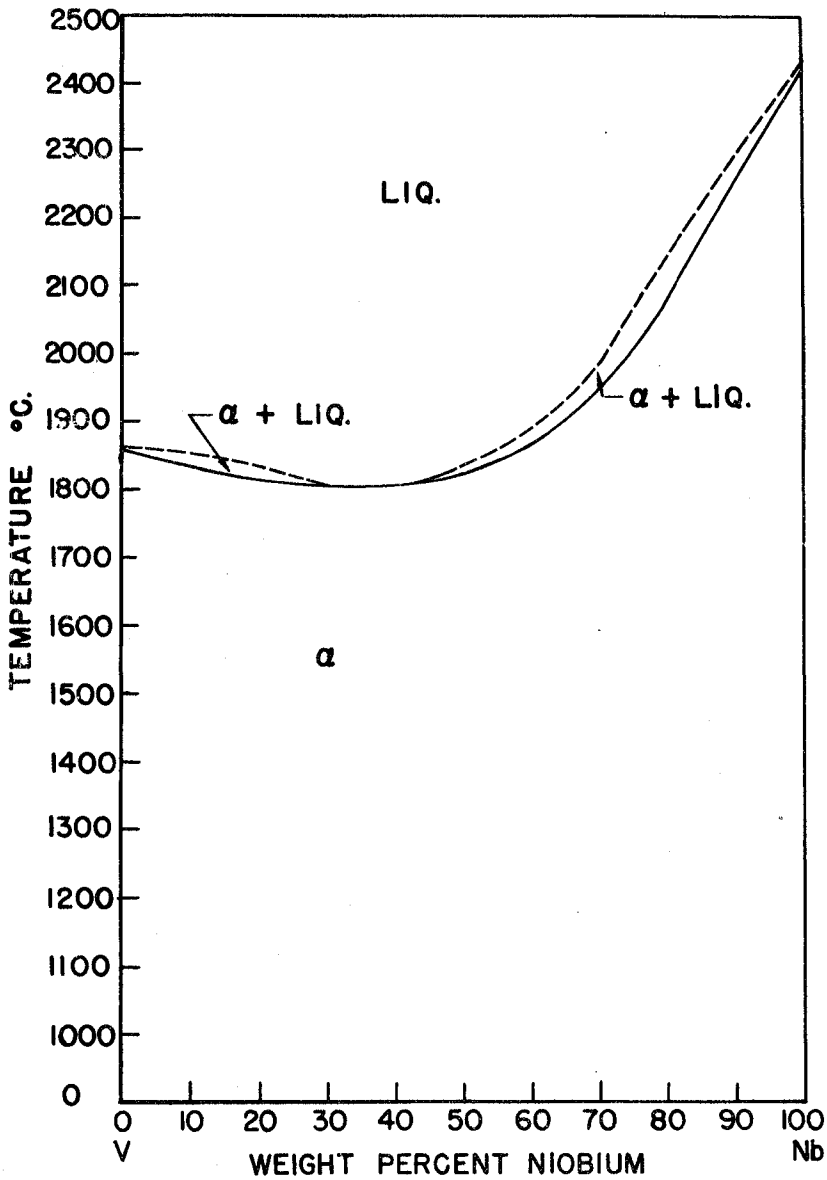

Fig. 38 Niobium-Vanadium Phase Diagram.

micrographs of arc melted niobium powder and niobium sheet respectively. The arc melted niobium powder (Figure 39) contains a considerable amount of a second phase that has been tentatively identified as mainly niobium carbide plus, perhaps, some niobium nitride and oxide, while the arc melted niobium sheet (Figure 40) is very nearly completely one phase. Several spurious lines were found on the X-ray pattern of the powdered niobium. One of these lines could be accounted for as due to niobium carbide or nitride (their lattice constants are almost identical) and the other line, while not due to niobium carbide, appeared in an X-ray diffraction pattern taken of niobium carbide. Since only one line was present for niobium carbide and this was in the front reflection region, no positive identification could be made of the impurity phase on the basis of X-ray evidence alone.

A chemical analysis of the niobium powder indicated that it contained approximately 1760 ppm. of carbon. Two specimens, one containing 0.2 per cent oxygen and the other 0.2 per cent carbon were prepared by adding niobium pentoxide or niobium carbide to high purity sheet niobium and arc melting. Figure 41 is a photomicrograph of the oxide contaminated niobium and Figure 42 is a photomicrograph of the carbide contaminated niobium. Since the second phase in the niobium powder somewhat resembles the second phase in the carbide contaminated niobium but does not resemble the oxide contaminated niobium, it has been concluded that the impurity in the niobium powder is mainly a niobium carbide and possibly niobium nitride. One other point

Fig. 39 Niobium Powder. (As arc melted. Second phase is impurities. Aqua regia plus 5% HF etch. X250).

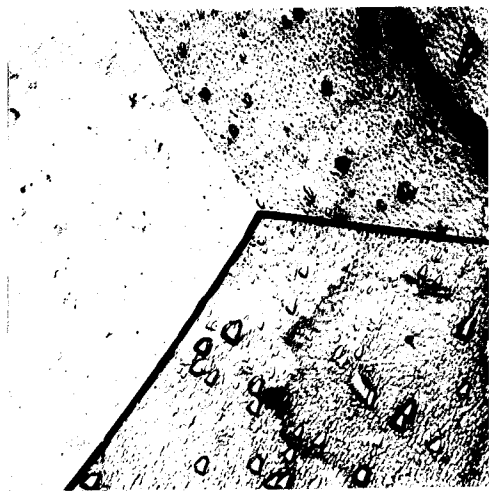

Fig. 40 Niobium Sheet. (As arc melted. Etching pits within grains. Aqua regia plus 5% HF etch. X250).

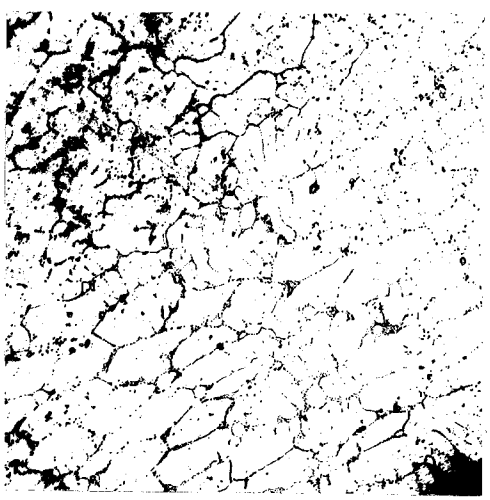

Fig. 41 Niobium Sheet Plus 0.2% Oxygen. (As arc melted. Aqua regia plus 5% HF etch. X250).

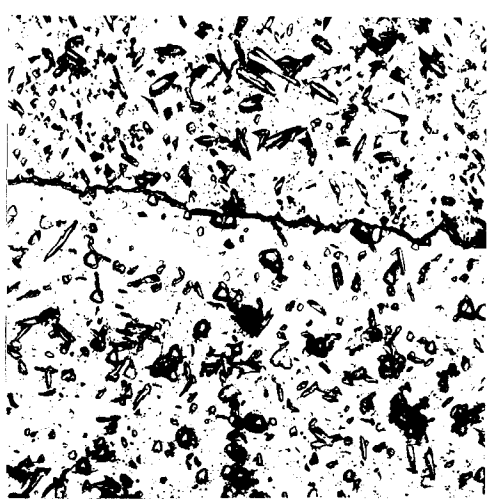

Fig. 42 Niobium Sheet Plus 0.2% Carbon. (As arc melted. Aqua regia plus 5% HF etch. X250).

might be made in support of the evidence that the second phase in the metal made with niobium powder is not oxide. Niobium oxide and niobium carbide have been shown to react at elevated temperatures forming niobium metal; therefore, since carbon is present in the arc melted niobium powder it is unlikely that much oxide can be present.

Figures 43 and 44 are photomicrographs of the bomb reduced vanadium that has been arc melted twice and in one case (Figure 44) has been annealed. The speckled areas within the grains are an impurity phase that is present in all vanadium that the author has seen. The larger spots in the grains of Figure 44 are impurities that were either picked up or agglomerated while annealing the specimen.

(b) Metallographic evidence. Figures 45 through 53 are photomicrographs of niobium-vanadium alloys spaced at 10 weight per cent intervals across the phase diagram starting at the vanadium rich end. The dark splotches that appear within the grains are etching pits and are quite common in vanadium, niobium, and their alloys. Figure 40, pure niobium, shows the etching pits very nicely, but in order to obtain sufficient contrast between the grains and grain boundaries it was necessary to etch the alloys so drastically that not only were etching pits formed but they are usually badly over etched before the grain boundaries appeared. All of these alloys contain only one phase except the 90 per cent niobium alloy (Figure 53) which contains a small amount of an impurity phase in the grain boundaries. This alloy

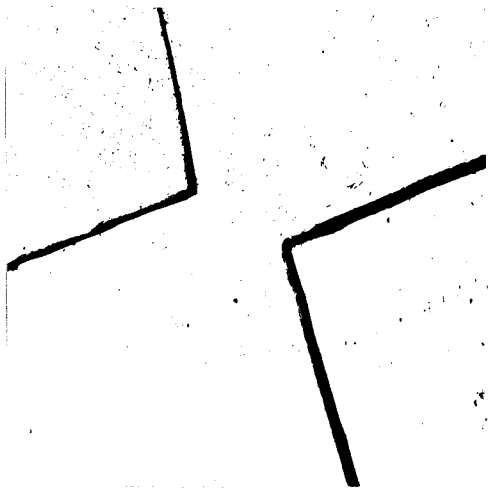

Fig. 43 Vanadium. (As arc melted. 2:1:1:1::HNO_3:H_2SO_4:HF:H_2O etch. X250).

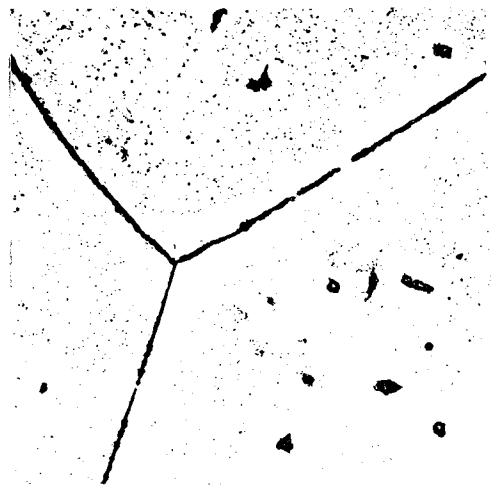

Fig. 44 Vanadium. (Annealed 40 hours at 1075°C. Same etch. X250).

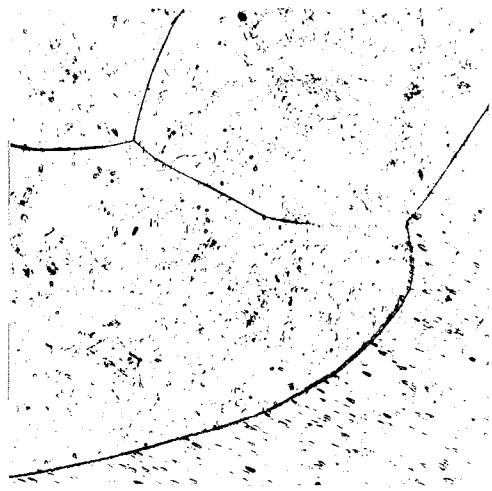

Fig. 45 10% Niobium. (As arc melted. Made with niobium powder. Same etch. X250).

Fig. 46 20% Niobium. (As arc melted. Made with niobium powder. Same etch. X250).

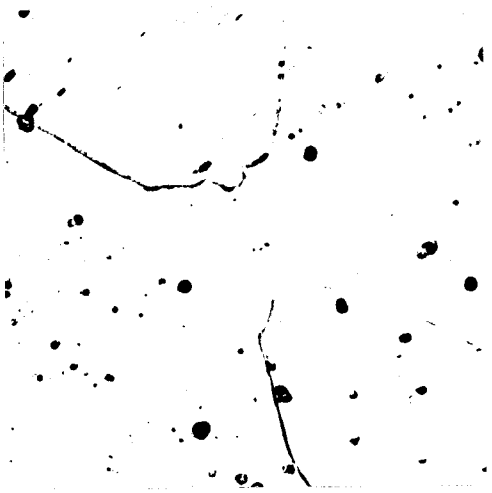

Fig. 47 30% Niobium. (As arc melted. Made with niobium powder. 2:1:1:1:: HNO_3:H_2SO_4:HF:H_2O etch. X250).

Fig. 48 40% Niobium. (As arc melted. Made with niobium powder. Same etch. X250).

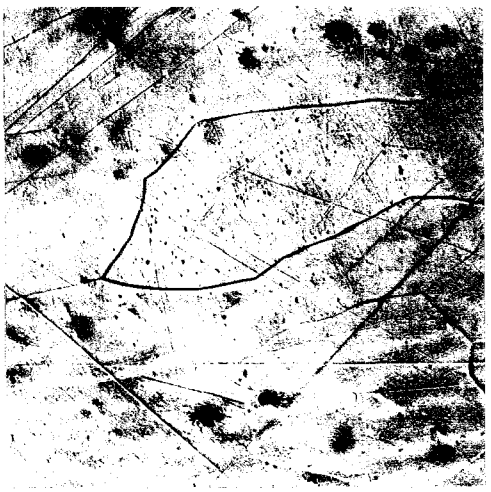

Fig. 49 50% Niobium. (As arc melted. Made with niobium powder. Same etch. X250).

Fig. 50 60% Niobium. (As arc melted. Made with niobium powder. Same etch. X250).

was made with powdered niobium and annealed 4 hours at 1600°C. and is typical of the appearance of alloys made with the powdered niobium and annealed at high temperatures.

Figures 54 through 58 are photomicrographs of several alloys made with either niobium sheet or niobium powder. These alloys have undergone several different annealing treatments. The alloys made with the niobium sheet (Figures 54, 55, and 56) have a much cleaner appearance than the alloys made with the niobium powder (Figures 57 and 58) that have undergone the same treatment. The small triangles in the grains of Figure 57 are again etching pits while the long black needles are an impurity phase that is quite common in the high vanadium alloys that were made using the niobium powder. It is interesting to note that the impurities shown in both Figures 57 and 58 are lined up along crystallographic planes. Since all of the alloys examined in this investigation contained only one metallic phase, photomicrographs have been presented for only a representative group. The annealing treatments and the appearances of all of the alloys investigated have been summarized in Table 10.

(c) X-ray evidence. From the results of microscopic examination of the alloys, it was quite certain that the niobium-vanadium alloy system was a complete series of solid solutions. To confirm this and to investigate the possibility of superlattice formation a series of X-ray diffraction patterns was taken of alloys separated by approximately 10 per cent increments across the phase diagram.

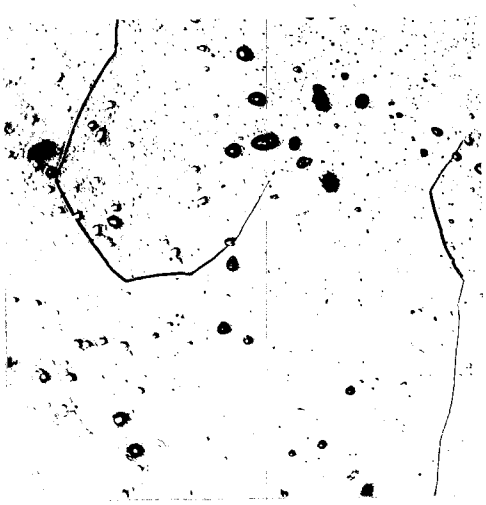

Fig. 51 70% Niobium. (As arc melted. Made with niobium sheet. 2:1:1:1::HNO_3:H_2SO_4:HF:H_2O etch. X250).

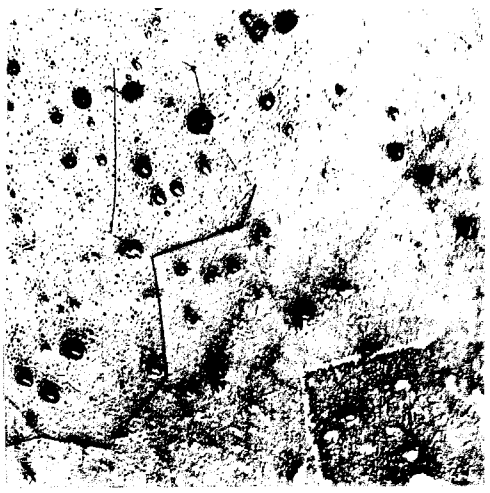

Fig. 52 80% Niobium. (As arc melted. Made with niobium sheet. Same etch. X250).

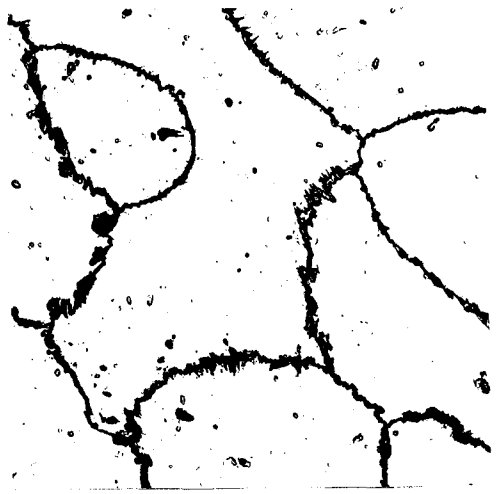

Fig. 53 90% Niobium. (Annealed 4 hours at 1600°C. Made with niobium powder. Impurities in grain boundaries. Same etch. X250).

Fig. 54 80% Niobium. (Annealed 40 hours at 1075°C. Made with niobium sheet. Same etch. X250).

Fig. 55 50% Niobium. (Annealed 40 hours at 1075°C. Made with niobium sheet. 2:1:1:1::HNO_3:H_2SO_4:HF:H_2O etch. X250).

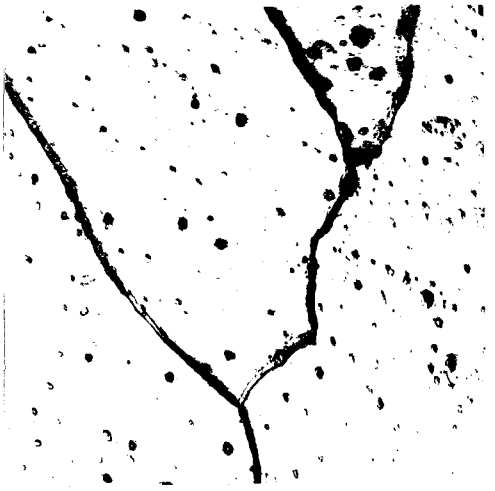

Fig. 56 30% Niobium. (Annealed 40 hours at 1075°C. Made with niobium sheet. Same etch. X250).

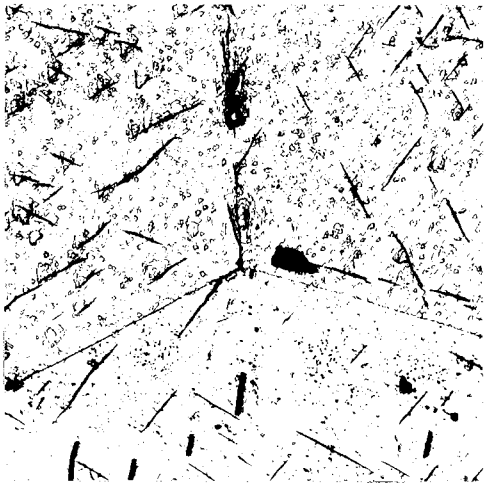

Fig. 57 10% Niobium. (Annealed 4 hours at 1500°C. Made with niobium powder. Needles of impurities within grains. Same etch. X250).

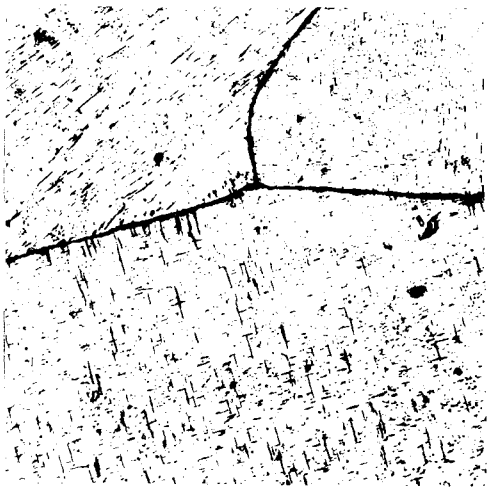

Fig. 58 30% Niobium. (Annealed 40 hours at 1075°C. Made with niobium powder. Impurity needles within grains. Same etch. X250).

Table 10. Results of Microscopic Examination

Composition % Nb	Source of niobium		Treatment of the alloy			
	Powder	Sheet	As arc melted	Annealed 40 hrs., 1075°C.	Annealed 4 hrs., 1500°C.	Annealed 4 hrs., 1600°C.
0			1	1		
5		x	1			
10		x	1	2		
10	x		1	2	2	
20		x	1	2		
20	x		1	2	2	
30		x	1	1		
30	x		1	2	1	
40		x	1	1		
40	x		1	2		3
50		x	1	1		
50	x		1	2		2
60		x	1	1		
60	x		1	3		1
70		x	1	1		
70	x		1	3		1
80		x	1	1		
80	x		1	3		3
90	x		1	3		3

[1]The alloy is one phase and clean in appearance, much like Figure 44.

[2]The alloy is one phase but contains impurities within the grains, much like Figure 56.

[3]The alloy is one phase but contains considerable amounts of impurities both in the grains and in the grain boundaries, much like Figure 37.

Since it was impossible to obtain good resolution in the back-reflection region on any of the alloys, which had been annealed 113 hours at 600°C., the X-ray pictures were taken on a Debye-Scherrer type camera.

Data (Table 11) obtained from X-ray measurements furnished further evidence supporting the contention that niobium forms a complete

Table 11. Lattice Constants of Niobium-Vanadium Alloys

Wt. % Nb	At. % Nb	Lattice constant, A°.
0.00	0.00	3.0288
10	5.54	3.0454
		3.0437
20	12.08	3.069
30	19.03	3.0836
40	26.77	3.1129
50	35.42	3.138
60	45.13	3.177
70	56.13	3.206
80	68.69	3.241
90	83.15	3.271
100	100	3.3079

series of solid solutions with vanadium. The data was corrected for film shrinkage using the method described in section II-B-3 of this report. The lattice constants were determined by extrapolating a° against the function

$$\frac{1}{2}\left(\frac{\cos^2\theta}{\sin\theta} + \frac{\cos^2\theta}{\theta}\right) \qquad (13)$$

which was arrived at experimentally by Nelson and Riley (31) and later put on a theoretical basis by Taylor and Sinclair (38). This extra-

polation has an advantage over the other extrapolations in general use in that it is linear over the range, θ = 10 to 90°. This allows the use of the low angle front reflections as well as the high angle reflections in the calculations of lattice constants and makes it feasible to obtain accurate lattice constants using Debye-Scherrer type cameras.

According to Vegard's law the lattice constant is a linear function of the atomic per cent in a binary solid solution. Consequently, if complete solid solubility exists in the niobium-vanadium alloy system, the plot (Figure 59) of the experimentally determined lattice constants against the atomic per cent niobium should be a straight line. This curve deviates slightly in the positive direction from the theoretical curve. Actually, this is not surprising as, in practice, very few solid solutions have been shown to exactly obey Vegard's law (39). However, since the curve is smooth and has no discontinuities, it is evident that no two phase region exists. If a two phase region did exist, a rather large discontinuity would be expected since the difference in atomic diameters between niobium and vanadium is significant, 8.5 per cent on the basis of Pauling's values of the atomic radii.

If a superlattice were formed, the X-ray patterns would be expected to contain extra lines corresponding to the superlattice structure. Since no extra lines were observed, it is probable that no ordering occurs in this alloy system.

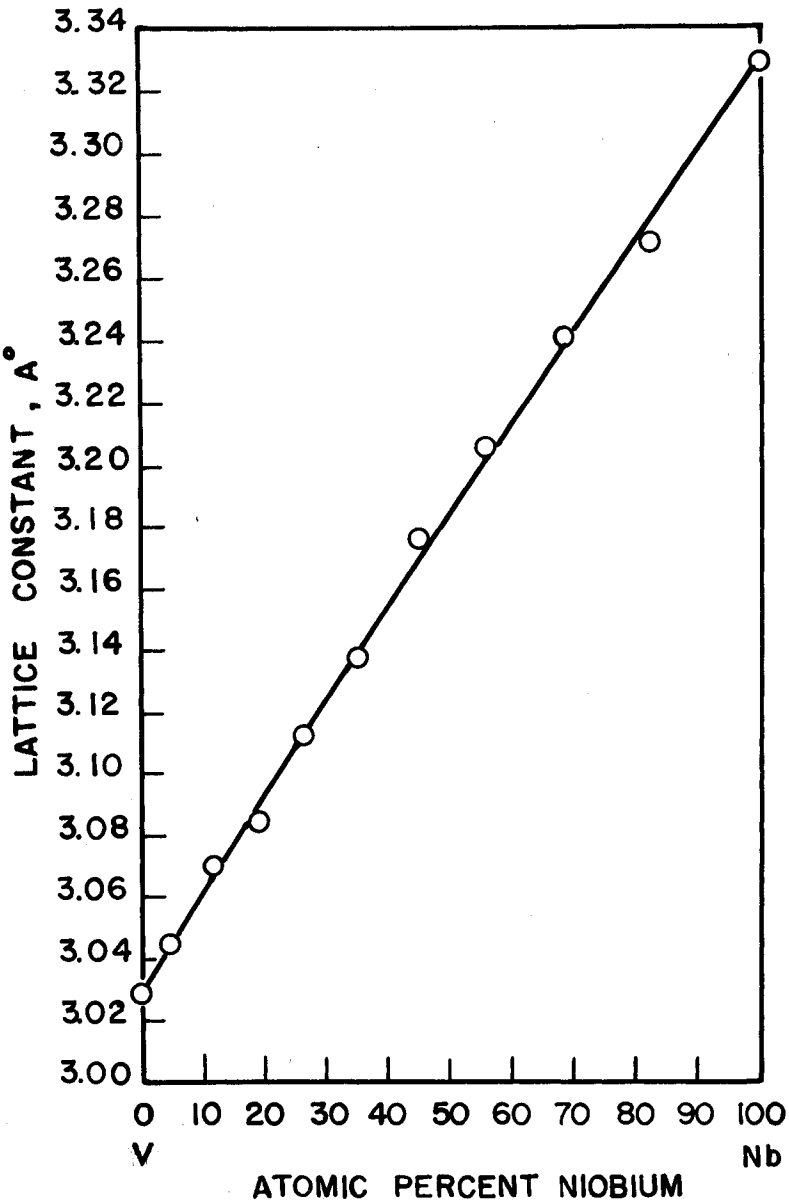

Fig. 59 Lattice Constant Versus Atomic Per Cent Niobium.

2. Determination of the solidus

The solidus curve for the niobium-vanadium alloy system has a long, nearly flat region extending from 10 to 50 per cent niobium. The minimum point is at about 30 per cent niobium and the minimum temperature is about 1805°C.

(a) Determination of approximate melting temperatures. Melting behaviors were observed on several of the alloys employing the method that was described in section III-B-3 of this report. It may be recalled that the sample was resting on an inverted graphite crucible while its melting was being observed. Evidently reactions occurred between the samples and the graphite forming some eutectic. In an attempt to prevent this reaction, a piece of niobium sheet was placed between the sample and the graphite. However, the graphite reacted with the niobium sheet which in turn reacted with the alloy and again a eutectic was formed between the alloy and the graphite. Figure 60 is a photomicrograph of the 20 per cent niobium alloy after it had been melted in contact with graphite and shows the eutectic that was formed.

An X-ray diffraction pattern was taken of this 20 per cent niobium alloy and all of the lines belonging to the original alloy were identified. In addition a series of lines belonging to a second phase, presumably the carbide, was present in the pattern.

(b) Melting bar method. The solidus curve (Figure 61) was established for the niobium-vanadium alloy system by determining melting temperatures of the alloys using the melting bar method. Most of the melting temperatures, obtained by this method, were taken on alloys

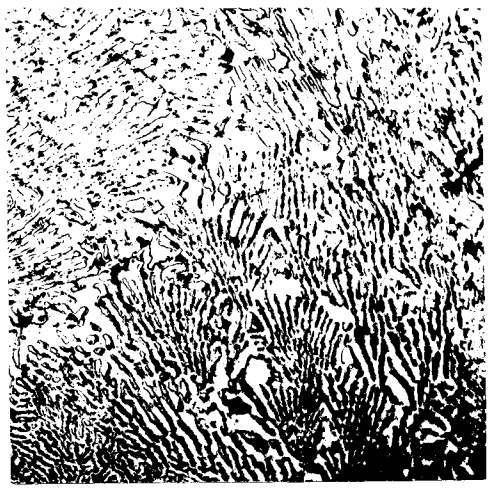

Fig. 60 20 % Niobium Melted in Contact with Graphite. (Eutectic structure. 2:1:1:1::HNO_3:H_2SO_4: HF:H_2O etch. X250).

prepared from sheet niobium since alloys made using the niobium powder could not be drilled if they contained more than 20 per cent niobium.

Vanadium has a vapor pressure of approximately 10 microns at 1800°C. according to Brewer (40). As a result of this vapor pressure, vanadium would distill from the alloys when they were held in the molten state for any length of time, and deposit as a film on the sight glass. Normally this film was very thin and had essentially no effect on the temperature readings, but occasionally, especially if the heating was

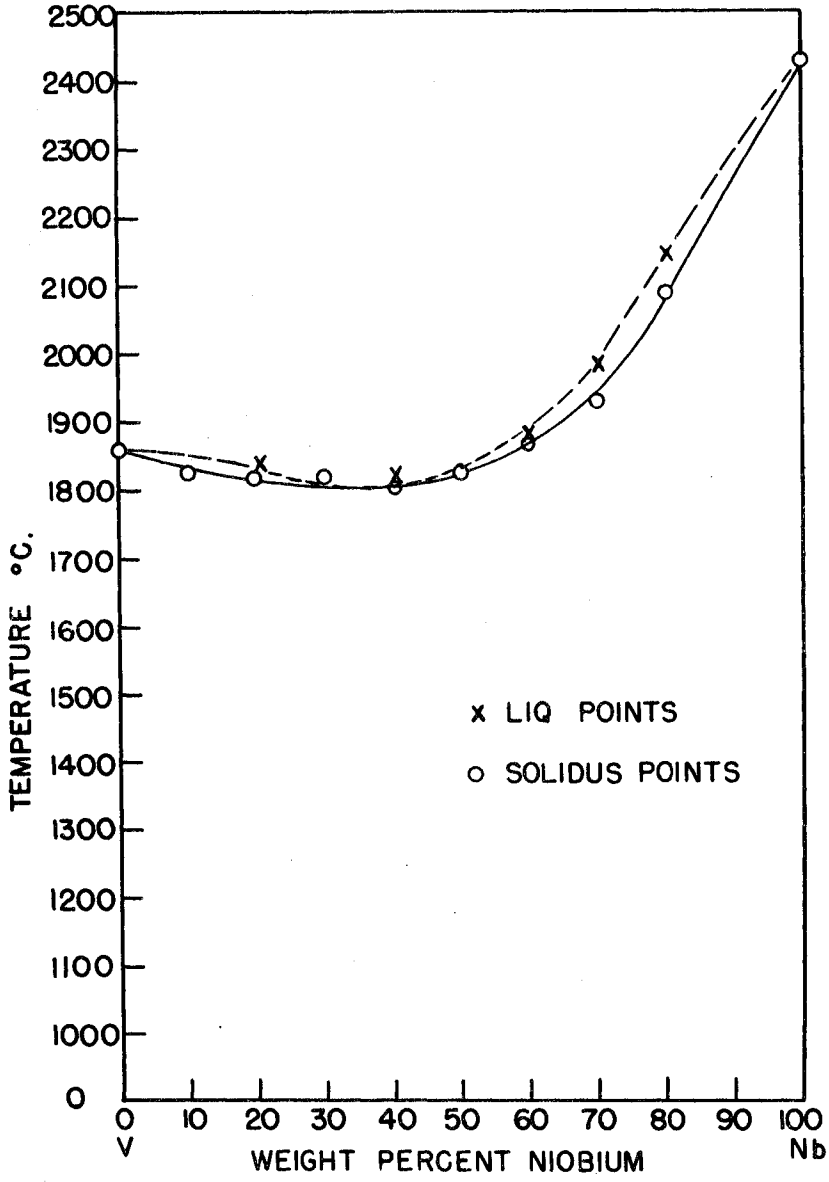

Fig. 61 Thermal Data, Niobium-Vanadium System.

continued after the alloy had started to melt, a heavy film was formed. Whenever a film was present on the sight glass after a melting temperature had been determined, a correction was made in the reading. The per cent transmission of the sight glass to light of 0.65 microns, the wave length of light for the optical pyrometer, was measured on a spectrophotometer. The temperature correction was then calculated for the absorption of light by the sight glass using the relationship

$$1/T - 1/T_a = \lambda \log A_\lambda / c_2 \log e \qquad (14)$$

where λ is 0.65 microns, c_2 is a constant having a value of 14,320 to 14,360, $A\lambda$ is the per cent transmission of the sight glass, T is the true absolute temperature, and T_a is the observed absolute temperature.

The reproducibility of the solidus melting points was very good and often the variation in solidus temperature was less than 5°C. on alloys of the same composition. Table 12 contains a summary of the solidus values that were determined by the melting bar method.

3. Determination of the liquidus curve

Several points on the liquidus curve of the niobium-vanadium alloy system were obtained incidental to the determination of the solidus points. In those instances where the hole in the melting bar did not fill immediately at the solidus point, the temperature of the specimen was slowly increased until the bar melted in two or the hole filled sufficiently to destroy the black body conditions. The tem-

Table 12. Solidus and Liquidus Temperatures

Alloy composition % Nb	Temperature liquid first appeared, °C.	Temperature the bar melted in two, °C.	Source of niobium used
0	1858		
	1861		
10	1765[a]		Powder
	1824		Powder
	1838		Sheet
20	1764[a]		Powder
	1813		Powder
	1819		Sheet
	1821	1840	Sheet
30	1811		Sheet
	1820		Sheet
40	1807	1812	Sheet
50	1821		Sheet
	1824		Sheet
	1850[b]		Sheet
60	1859		Sheet
	1864	1874	Sheet
70	1928	1928[c]	Sheet
	1929	1980	Sheet
80	2090	2140	Sheet
100	2421		Powder

[a]The bar melted out of the hole; reading is low.

[b]The melting was not observed when it started; reading is high.

[c]The bar broke rather than melted in two.

perature at which the bar melted in two was taken as an indication of the liquidus temperature, and in no case was the temperature at which liquid first appeared separated from this temperature by more than 50°C. In the nearly flat region of the solidus curve essentially no difference in temperature was noticed between the first appearance of liquid and the point at which the bar melted in two. However, since the bars melted in two so rapidly, the liquidus probably lies very little above the solidus throughout most of the flat region of the solidus cruve. The actual liquidus points obtained have been listed in Table 12 and both solidus and liquidus points have been plotted on the drawing of the phase diagram shown in Figure 61.

4. Physical properties of niobium-vanadium alloys

As may have been gathered from the preceding discussions, the type of niobium used for alloy preparation has a tremendous effect on the physical properties of niobium-vanadium alloys. Alloys made with the niobium powder that contain over 10 per cent niobium are very brittle and difficult to machine, drill, or deform without fracturing. The 10 per cent niobium alloy could be hammered without fracturing, but it could not be cold rolled more than a few per cent without shattering.

On the other hand alloys made from niobium sheet were very malleable and easy to machine. All of the melting bars were drilled with a number 63 drill with no difficulty and alloys were sampled for chemical analysis by milling the surfaces of the alloys. Arc melted

alloys containing 5, 10, and 40 per cent niobium (sheet) were successfully cold rolled to 10 mil sheet, over a 90 per cent reduction, without serious edge cracking and with no annealing.

Hardness values were measured on most of the alloys, both as arc melted and after annealing, using a Rockwell hardness tester with a "Brale" indentor and a 60 kilogram load. The Rockwell "A" hardness numbers versus the composition in weight per cent niobium have been plotted in Figure 62. In all cases the curves have a flat maximum and the alloys made with powdered niobium were considerably harder than those made from niobium sheet, especially in the high niobium region. Annealing seemed to cause very little change in the hardness in most cases.

Since both niobium and vanadium are corrosion resistant metals, several corrosion tests were made on niobium-vanadium alloys. All of the corrosion tests were made in a sealed stainless steel bomb. The alloys were wrapped separately in stainless steel screen, placed in the bomb and covered with distilled water; the bomb was then sealed by means of a metal gasket and screw cap.

The first test was made at 178°C. for 125 hours. Vanadium and alloys containing 5, 10, and 40 per cent niobium were included in this test. The appearances of the corrosion specimens were almost the same after the test as before the test. Since there was so little change, the alloys were put back in the bomb and the test at 178°C. was continued for an additional 250 hours. Outside of a slight greyish surface film, there was no apparent change in the appearance

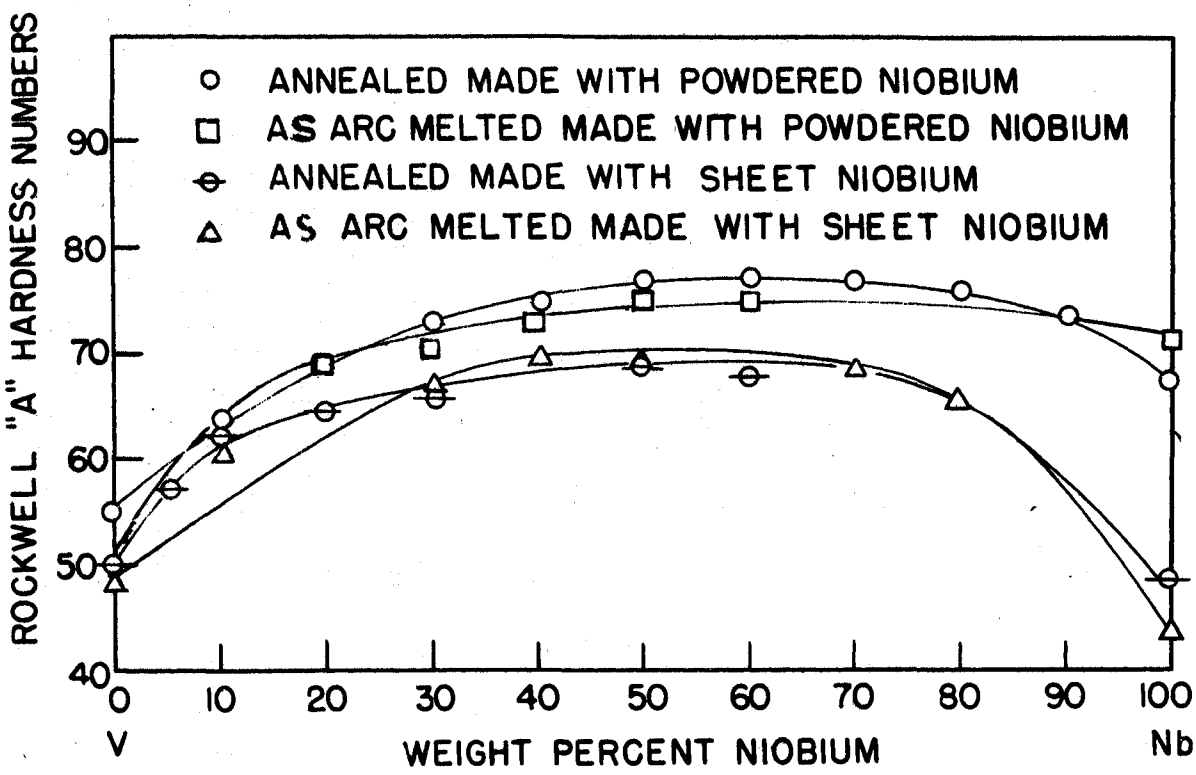

Fig. 62 Hardness Values, Niobium-Vanadium System.

of the specimens after this test. The weight changes of the specimens were within the experimental error of weighing (0.0003 grams).

After the test at 178°C. the film on the specimens was removed by fine grinding. These alloys along with two samples of niobium were placed in the bomb and heated at 250°C. for 50 hours. Except for the vanadium specimen, which was covered with a very black film, the alloys were covered with a thin, tightly adhering film that was greyish colored. The 40 per cent niobium alloy was still shiny in appearance in certain areas and had an insignificant change in weight.

The film was again removed from the specimens by grinding and the specimens returned to the bomb. They were heated at 330°C. for 60 hours. All of the specimens were covered with a black film upon the conclusion of this test. The film on the vanadium specimen and the 5 per cent alloy had started to powder slightly, while the films on the other alloys were still quite intact.

On the basis of these tests, it has been concluded that niobium-vanadium alloys have a slow corrosion rate in hot distilled water. It appears that the addition of niobium to vanadium definitely increases the water corrosion resistance of vanadium at temperatures up to 330°C.

IV. SUMMARY

The niobium-thorium alloys have been shown to belong to a eutectic type system having no intermediate phases. The eutectic formed between niobium and thorium is at about 8 weight per cent niobium. The composition of the eutectic was assigned on the basis of metallographic evidence. Further evidence supporting this eutectic composition was obtained by extrapolating the experimentally determined thorium rich liquidus curve to the eutectic horizontal. On the basis of melting bar studies, thermal analysis, and resistance measurements, the eutectic temperature has been found to be about 1435°C.

Since no change in the lattice parameter of niobium was observed upon the addition of thorium, the solubility of thorium in solid niobium is considered negligible. On the basis of precision X-ray data, the solubility of niobium in β thorium is less than 0.1 per cent. The extent of solid solubility of niobium in β thorium is believed to be less than 1 per cent. Metallographic examination and the fact that a eutectic melting temperature was observed on a 1 per cent niobium alloy support this latter contention.

Niobium lowers the reported α - β transformation temperature 1408°C. of thorium slightly. This lowering might be associated with a scavenging effect of niobium or the formation of a eutectoid in that region of the phase diagram involving less than 1 per cent niobium. Although no microscopic evidence of a eutectoid structure could be

retained in these alloys the possibility of a eutectoid is not ruled out.

Niobium and vanadium have been shown, by means of metallographic examination and X-ray studies, to form a complete series of solid solutions. The solidus curve of the niobium-vanadium alloy system has a long, nearly flat, section extending from about 10 to 50 per cent niobium. The curve passes through a minimum at about 35 weight per cent niobium and the minimum temperature is approximately 1805°C. The liquidus curve lies very close to the solidus curve throughout the entire alloy system. In no instance was a temperature difference of more than 50°C. observed between the solidus and the liquidus for the same alloy. In the region of the minimum the liquidus curve appears to be almost identical with the solidus curve.

Niobium-vanadium alloys prepared using the niobium powder were brittle and very difficult to machine. These alloys could be drilled only if they contained less than about 30 per cent of this niobium. All attempts at cold rolling these alloys resulted in the almost immediate fracture of the specimen. On the other hand, niobium-vanadium alloys made using niobium sheet were very easy to machine. Holes as small as 0.031 of an inch were readily drilled into these alloys. The alloys made with the sheet niobium could be cold rolled to thin sheet without annealing and without serious edge cracking. Reductions of over 90 per cent in thickness were readily obtainable on the niobium-vanadium alloys made with niobium sheet.

Niobium, vanadium and the alloys containing 5, 10, and 40 per cent niobium withstood corrosion tests of 375 hours at 178°C., 50 hours at 250°C., and 60 hours at 330°C. without being seriously attacked. Only after the test at 330°C. were any of the specimens covered with a heavy film. The 5 per cent niobium alloy was coated with a black film that had started to powder slightly. The vanadium specimen in this test had been attacked to about the same extent as the 5 per cent niobium alloy. The remainder of the specimens were covered with a tightly adhering, black film.

Before the experimental work was started on the niobium-thorium and the niobium-vanadium alloy systems, predictions were made on the basis of the Hume-Rothery rules as to the types of phase diagrams to be expected for these alloy systems. The niobium-thorium alloy system was expected to be a eutectic system with very limited solid solubility with a possibility of intermediate phase formation. The niobium-vanadium system was expected to be a complete series of solid solutions. The solidus curve of the niobium-vanadium alloy system was expected to pass through a minimum. A comparison of the predicted diagrams and the experimentally determined diagrams revealed that both alloy systems came definitely within the scope of the predictions.

V. ACKNOWLEDGMENTS

The author especially wishes to express appreciation to Dr. H. A. Wilhelm for his helpful counsel in connection with this investigation. The author is also indebted to Dr. O. N. Carlson for his suggestions and advice, to Mr. G. Muller for his capable and cooperative assistance in the experimental work, and to the entire metallurgy group for their suggestions and cooperation in this work.

The chemical analyses were performed by the analytical section of the laboratory under the direction of Dr. C. V. Banks.

The author also wishes to thank Mr. C. Finch for preparing the many unusual ceramics necessary to the investigation.

The author is indebted to the Ames Laboratory of the Atomic Energy Commission for the funds and facilities made available for this research.

VI. LITERATURE CITED

1. Pauling, L. J. Am. Chem. Soc., 69, 542 (1947).

2. Pauling, L. "The Nature of the Chemical Bond," p. 60, 2nd ed., Ithaca, New York, Cornell University Press. 1948.

3. Oriani, R. A. Report No. RL-578, Schenectady, New York, General Electric Research Lab., Aug. 1951. Multigraphed.

4. Gordy, W. Phys. Rev., 69, 604 (1946).

5. Hume-Rothery, W. "The Structure of Metals and Alloys," London, England, Institute of Metals. 1936.

6. Hume-Rothery, W. and G. V. Raynor Phil. Mag., 26, 129, 143, 152, (1938).

7. Hildebrand, J. H. and Scott, R. L. "Solubility of Nonelectrolytes," p. 333, 3rd ed., New York, Reinhold Publishing Corp. 1950.

8. Hildebrand, J. H. and Scott, R. L. "Solubility of Nonelectrolytes," p. 427, 3rd ed., New York, Reinhold Publishing Corp. 1950.

9. Carlson, O. N. Private Communication, 1952.

10. Lange, A. L. "Handbook of Chemistry," p. 66, 6th ed., Sandusky, Ohio, Handbook Publishers, Inc. 1946.

11. Hodgman, C. D. "Handbook of Chemistry and Physics," p. 287, 30th ed., Cleveland, Ohio, Chemical Rubber Publishing Co. 1948.

12. McKinstry, H. E. "Mining Geology," p. 598, New York, Prentice-Hall Inc. 1948.

13. Metals Handbook Committee, "Metals Handbook," p. 19, Cleveland, Ohio, American Society for Metals. 1948.

14. Metals Handbook Committee, "Metals Handbook," p. 1137, Cleveland, Ohio, American Society for Metals. 1948.

15. Lange, A. L. "Handbook of Chemistry," p. 191, 6th ed., Sandusky, Ohio, Handbook Publishers, Inc. 1946.

16. Dushman, S. "Scientific Foundations of Vacuum Technique," p. 749, New York, John Wiley and Sons. 1948.

17. Lange, A. L. "Handbook of Chemistry," p. 82, 6th ed., Sandusky, Ohio, Handbook Publishers, Inc. 1946.

18. Winchell, A. N. "Elements of Mineralogy", p. 309, New York, Prentice-Hall, Inc. 1942.

19. "Project Handbook," Vol. III, Chap. IX, Classified Publication, Atomic Energy Commission (1946).

20. Thompson, J. G. Metals and Alloys, 4, 114 (1933).

21. Peterson, D. and Michelson, R. Unpublished Research, Ames Lab. of Atomic Energy Commission (1953).

22. Chiotti, P. ISC., Classified Report, Atomic Energy Commission (Jan., Feb., and Mar. 1953).

23. Goldhoff, R. BMI.-89 Classified Report, Atomic Energy Commission (Sept., 1951).

24. Frye, J. H. ORNL.-754, Classified Report, Atomic Energy Commission (June, 1950).

25. Rogers, B. A. ISC.-200, Classified Report, Atomic Energy Commission (Jan., 1952).

26. Foote, F. G. CT-2794, Classified Report, Atomic Energy Commission (Sept., 1951).

27. Bradley, A. J. and Jay, A. H. Proc. Phys. Soc., 44, 563 (1933).

28. Pirani, M. and Alterthum, H. Z. Elektrochem., 29, 5 (1923)

29. Foote, P. D., Fairchild, C. A., and Harrison, T. R. "Pyrometry Practice," Nat. Bur. Standards Tech. Paper No. 170, p. 170, 1921.

30. Chiotti, P. Unpublished Ph.D. Thesis, Ames, Iowa, Ames Lab. of Atomic Energy Commission (1952).

31. Nelson, J. M. and Riley, D. P. Proc. Phys. Soc. (London) 57, 160, (1945).

32. Sefstrom, N. G. Pogg. Ann., 21, 43 (1931).

33. Roscoe, H. E., Phil. Trans., 159, 679 (1869).

34. McKinstry, H. E. "Mining Geology," p. 601, New York, Prentice-Hall, Inc. 1948.

35. Powers, R. M. Unpublished Ph.D. Thesis, Ames, Iowa, Ames Lab. of Atomic Energy Commission (1952).

36. McKechnie, R. K. and Seybolt, A. U. J. Electrochem. Soc., 97, 311 (1950).

37. Long, J. R. Unpublished Thesis, Ames, Iowa, Ames Lab. of Atomic Energy Commission (1951).

38. Taylor, A. and Sinclair, H. Proc. Phy. Soc. (London) 57, 108, (1945).

39. Barrett, C. S. "Structure of Metals," p. 202, New York, McGraw Hill Book Co., Inc. 1943.